Oligocene-Miocene drainage evolution of NW Borneo: stratigraphy, sedimentology and provenance of Tatau-Nyalau province sediments

H. Tim Breitfeld [a*], Juliane Hennig-Breitfeld [a], Marcelle K. BouDagher-Fadel [b], Robert Hall [a], Thomson Galin [c]

[a] *SE Asia Research Group, Department of Earth Sciences, Royal Holloway University of London, Egham, TW20 0EX, UK*

[b] *Department of Earth Sciences, University College London, London, WC1H 0BT, UK*

[c] *Minerals and Geoscience Department Malaysia (JMG) Sarawak, Jalan Wan Abdul Rahman, Kenyalang Park P.O. Box 560 93712 Kuching, Sarawak, Malaysia*

*Corresponding author: tim.breitfeld@rhul.ac.uk

Abstract

Clastic sediments of Oligocene to Lower Miocene age form a major thick and widespread sequence in the Tatau-Nyalau province of the north Sarawak Miri Zone. New light and heavy mineral data, U-Pb detrital zircon geochronology and biostratigraphy are used to identify the age, depositional environment, provenance and potential sources of sediment to reconstruct the drainage evolution of NW Borneo. Based on the biostratigraphic ages, depositional environments and provenance characteristics we modify previous stratigraphy and divide the Oligocene to Lower Miocene sequences into the Nyalau Formation (Biban Sandstone Member and Upper Nyalau Member), Kakus Unit, and Merit-Pila Formation. Two dominant source provinces were identified: the Malay-Thai Tin Belt which supplied sediments dominated by Permian-Triassic zircons, and the Schwaner Mountains of central Borneo which is identified by abundant Cretaceous zircons. Sediments either came directly, or were recycled from older sedimentary rocks, from these sources. The Sunda River deposited the Nyalau Formation during the Oligocene to Early Miocene with a dominant Malay-Thai Tin Belt source. The

Merit-Pila Formation of the Sibu Zone was deposited contemporaneously by a proto-Rajang River that drained Central Borneo (recycling the Rajang Group and Schwaner granitoids). Between c. 17 Ma the Sunda River system terminated and sedimentation was dominated by the northward prograding proto-Rajang River delta, depositing the Kakus Unit in the Miri Zone. This drainage system was active until the Late Miocene, before further uplift of Borneo terminated most sedimentation in the onshore part of present-day Borneo.

Keywords: NW Borneo; Miri Zone; Nyalau Formation; Provenance; Detrital zircon geochronology; Paleodrainage evolution, Sunda River Delta

1. Introduction

The Nyalau Formation of NW Borneo (Fig. 1) covers an area of c. 11550 km^2 near the coast of North Sarawak within the Miri Zone of Haile (1974) and has been correlated with offshore deltaic to fluvial deposits which form important hydrocarbon reservoirs. The formation has been assigned a wide age range from Early Oligocene to Early Miocene (Kirk, 1957; Liechti et al., 1960; Wolfenden, 1960; Kho, 1968). Previous investigations on land reported lithostratigraphic variations used to distinguish different members although these were not consistently used (e.g. Liechti et al., 1960; Wolfenden, 1960) and often only the term Nyalau Formation is used (e.g. Hutchison, 2005). Hassan et al. (2013) presented a very detailed facies and environment interpretation of the Nyalau Formation in the Bintulu area (Fig. 2), but no other exposures in the Miri Zone were discussed. The Nyalau Formation has also been identified as outliers c. 100 km further south in Central Sarawak (Sibu Zone) (Fig. 2), but correlation with the type area in North Sarawak is uncertain. The Nyalau Formation and other formations of the Miri Zone have equivalents in the sub-basins of offshore Sarawak (Fig. 1) where the stratigraphy has been subdivided into cycles (Hageman, 1987; Hageman et al., 1987). The Nyalau Formation has been considered equivalent to mainly Cycles I and II (Hutchison, 2005). Understanding the onshore geology can help to understand the onshore region.

We present new light and heavy mineral data, U-Pb detrital zircon geochronology, field observations and micropalaeontology for the Nyalau Formation and associated formations and propose some revisions of stratigraphy. Combined with earlier work, these new data are used to distinguish Oligocene and Lower Miocene formations and members, to determine their ages, provenance and environments of deposition, and to draw conclusions about the palaeodrainage evolution of NW Borneo.

2. Geological setting of NW Borneo

2.1. Tectono-stratigraphic zones

NW Borneo (Fig. 1) has been subdivided on land into four major zones (Haile, 1974). The southernmost zone includes Cretaceous metamorphic and igneous rocks assigned to the SW Borneo basement, and in part to the West Borneo province (Hennig et al., 2017a). Further north, the Kuching Zone is characterised by a heterogeneous basement composed of Mesozoic crystalline and Paleozoic to Mesozoic (meta-) sedimentary rocks which are mostly overlain by lower Paleogene terrestrial to marginal marine deposits (Liechti et al., 1960; Williams et al., 1988; Doutch, 1992; Hennig et al., 2017a; Breitfeld et al., 2017, 2018). The Kuching Zone is separated from the Sibu Zone to the north by the Lupar Line. The Sibu Zone is composed mainly of sediments of the Rajang Group, which are the deep marine equivalent of the Kuching Zone sedimentary rocks (Galin et al., 2017; Breitfeld and Hall, 2018). The basement is not exposed. Finally, the Miri Zone is north of the Sibu Zone, and separated from it by the Bukit Mersing Line (Fig. 1). It includes Oligocene to Miocene fluvio-deltaic, tidal and marine deposits that are unconformably above Paleogene deep marine deposits of the Rajang Group. The Nyalau and Setap Shale Formations are the most extensive and thickest deposits of the Miri Zone (Figs. 2 and 3; Liechti et al., 1960).

2.2. Tectonic history in the Cenozoic

The Rajang Group formed a large submarine fan system at the eastern Sundaland margin during the latest Cretaceous to late Eocene (Galin et al., 2017; Breitfeld and Hall, 2018). Deposition of the Rajang Group ended at c. 37 Ma and it was uplifted, eroded and later subsided to form the basement of the Miri Zone successions (Hennig-Breitfeld et al., 2019, in press). This tectonic event is marked by the Rajang Unconformity that separates the marine Rajang Group from overlying terrestrial to shallow marine deposits. Above the Rajang Unconformity in the southern Miri Zone are predominantly fluvio-deltaic and tidally influenced sediments that have previously been assigned to the Buan and Nyalau Formations (Liechti et al., 1960). Further north, the argillaceous marine Setap Shale Formation with isolated limestone reefs is dominant (Liechti et al., 1960; Hennig-Breitfeld et al., 2019) and is contemporaneous with the Nyalau Formation (Hutchison, 2005). The Nyalau Unconformity (Hennig-Breitfeld et al., 2019) separates these formations (Fig. 3) from overlying Neogene tidal to fluvio-deltaic sediments that have been assigned to various formations (e.g. Begrih, Lambir, Miri Formations).

Equivalent sediments in offshore Sarawak have been divided into seven cycles that extend from the Oligocene to the Pleistocene and include open marine, coastal plain, fluvio-marine, and deltaic deposits (Hageman, 1987). The age ranges for Cycles I to V are broadly similar to the Miri Zone successions onshore, and Cycles I and II have been correlated with the Nyalau Formation (e.g. Hutchison, 2005).

2.3. Tatau-Nyalau province and the Sunda River Delta

We use the term Sunda River Delta for the palaeo-delta that developed in the Early Oligocene above the Rajang Group containing predominantly tidal and fluvio-deltaic sedimentary rocks and their marine equivalents, and bounded at the base by the Rajang unconformity and at the top by the Nyalau Unconformity. In onshore NW Borneo the majority of these sediments are parts of the Tatau and Nyalau Formations and we use the term Tatau-Nyalau province for the region. We have revised the Tatau-Nyalau Basin stratigraphy and this is discussed in detail below. In addition to the Tatau and Nyalau Formations, the Sunda River Delta deposits also include other formations including the Setap Shale Formation and Sibuti Formation (as pro-delta deposits), and the Buan Formation.

3. Sampling and methodology

Fieldwork in the Miri Zone was carried out along roads around the towns of Tatau, Bintulu, Similajau and Batu Niah (Fig. 2) and in the Sibu Zone by boat along the Rajang River north of the town of Kapit (Fig. 2). 17 samples were collected; 13 from the Nyalau Formation, Merit-Pila Formation and Kakus Unit (previously the latter two were mapped as the Nyalau Formation), two from the Setap Shale Formation and two from the Subis Limestone of the Tangap Formation. Ten arenaceous samples of the Nyalau Formation, Merit-Pila Formation and Kakus Unit were analysed for light mineral compositions, and from seven of these samples heavy mineral compositions and detrital zircon U-Pb ages were obtained. Seven limestone samples from the Subis Limestone, the Setap Shale Formation and the Nyalau Formation yielded benthic or planktonic foraminifera that were analysed for age and depositional environment.

3.1. Light mineral analysis

For light mineral modal analysis, the point counting method of Gazzi-Dickinson was used (e.g. Dickinson et al., 1983). 500 points were counted per sample, which resulted in the count of at least 400 framework grains. Grains smaller than 30 µm cannot be optically resolved and were assigned to matrix (Ingersoll et al., 1984; Pettijohn et al., 1987). Porosity was not measured. Sodium cobaltinitrite was used for staining alkali feldspar and barium chloride and amaranth solution were used for staining plagioclase.

3.2. Heavy mineral sample preparation

Sample preparation for heavy mineral analyses and zircon enrichment was carried out at Royal Holloway University of London. A 63-250 µm fraction was used for geochronology and heavy mineral analysis.

Indurated samples were crushed to gravel-sized chips using a jaw crusher and more friable samples were processed by mortar and pestle. Heavy minerals were separated by using standard heavy liquid lithium heteropolytungstate at a density of 2.89 g/cm^3. They were identified optically (Mange and Maurer, 1992) and also analysed using a scanning electron microscope and energy-dispersive X-ray spectroscopy (EDS). Between 334 and 812 grains (translucent and opaque) were counted for the individual samples. Most samples yielded between 380 and 600 translucent grains. For sample TB51 only 260 translucent heavy minerals could be counted. Heavy mineral abundances below 1 % of the heavy mineral assemblage are reported as trace.

Zircon concentrates were further processed with a FRANTZ magnetic barrier separator and then immersed into di-iodomethane at 3.3 g/cm^3 to maximise the purity of the zircon separates. Zircon grains were imaged in transmitted light to detect cracks or inclusions. Cathodoluminescence imaging was performed for each grain to identify zoning and guide selection of analysis spots for the laser ablation inductively coupled plasma mass spectrometry (LA-ICP-MS).

3.3. Geochronology

3.3.1. LA-ICP-MS U-Th-Pb dating

U-Pb LA-ICP-MS analysis was performed at Birkbeck College, University of London with a New Wave NWR 193 nm laser ablation system coupled to an Agilent 7700 quadrupole-based plasma ICP–MS with a two-cell sample chamber. A spot size of 25 µm was used for the ablation. The Plešovice zircon standard (337.13 ± 0.37 Ma; Sláma et al., 2008) and a NIST 612 silicate glass bead (Pearce et al., 1997) were used to correct for instrumental mass bias and depth-dependent inter-element fractionation of Pb, Th and U. Data reduction was achieved with the GLITTER software (Griffin et al., 2008). The data were corrected using the common lead correction method of Andersen (2002), which is used as a ^{204}Pb common lead-independent procedure.

The age obtained from the ^{207}Pb/^{206}Pb ratio is given for grains older than 1000 Ma. For ages younger than 1000 Ma, the ages obtained from the ^{238}U/^{206}Pb ratio are given because ^{207}Pb cannot be measured with sufficient precision, resulting in large analytical errors (Nemchin and Cawood, 2005). Concordance was tested by using a 10 % threshold between the ^{207}Pb/^{206}Pb and ^{206}Pb/^{238}U ages for ages greater than 1 Ga and between the ^{207}Pb/^{235}U and ^{206}Pb/^{238}U ages for ages below 1 Ga. Age histograms and probability density plots were created using an R script that adopts the approach of Sircombe (2004) for calculating probability density. Where cores and rims were observed in CL images, both sites were analysed following the approach by Zimmermann et al. (2018) in order to detect all age peaks, which is important for provenance studies. However, a core-rim age differences were only observed in a few grains. Analytical results are presented in Supplementary Tab. 1.

4. Stratigraphy and sedimentology

Previous studies (Liechti et al., 1960; Wolfenden, 1960) identified a major unconformity in Sarawak above the Rajang Group within the deep marine Tatau Formation. Based on new field-based investigations, and considering the results of the 1960 studies, Hennig-Breitfeld et al. (2019) proposed a different position for this unconformity and revised the stratigraphic terminology for the upper Rajang Group and overlying strata (Figs. 2 and 3).

What previously was called Tatau Formation (Liechti et al., 1960; Wolfenden, 1960) north of the Bukit Mersing Line included deep marine turbidites, volcanics and limestones in the Pelugau-Arip valleys, above the deep marine Rajang Group. An unconformity was interpreted, but not observed, by these authors within the Tatau Formation. Hennig-Breitfeld et al. (2019) proposed that the major unconformity, the Rajang Unconformity, was not within, but at the top of these deep and open marine deposits. They therefore assigned those rocks to the uppermost member of the Rajang Group, the Bawang Member, which includes steeply dipping turbidites, acid Arip Volcanics, and interbedded discontinuous limestones named informally the Arip Limestones. The Tatau Formation was redefined by Hennig-Breitfeld et al. (2019) to include only the gently dipping sediments above the Rajang Unconformity. The oldest sediments of the Tatau-Nyalau province, above the Rajang Unconformity, are conglomerates and sandstones of the Rangsi Conglomerate which form the lower Tatau Formation, overlain by fluvio-deltaic sediments of the upper Tatau Formation (Hennig-Breitfeld et al., 2019, in press). The Rangsi Conglomerate was previously also interpreted as Neogene (Liechti et al., 1960; Mat-Zin, 2000), however detailed research by Wong (2011) supports the Early Oligocene age and stratigraphic position at the base of the Tatau Formation. Conformably above the Tatau Formation is the shale-dominated, littoral, inner neritic to neritic sediments of the Buan Formation, which locally rests unconformably on the Bawang Member (Liechti et al., 1960).

Rocks formerly assigned to the Nyalau Formation by Liechti et al. (1960) are the subject of this paper. They conformably overlie the Buan Formation and comprise Oligocene to Lower Miocene clastic deposits, which Liechti et al. (1960) divided into the Biban Sandstone Member, an undifferentiated middle part (Nyalau Formation in general), and Kakus Member. Liechti et al. (1960) commented that the top of this sequence "…the delimitation of the Nyalau Formation, especially its Kakus Member, from the Belait or Lambir Formation is one of the most vexing problems of the stratigraphy…". Based on our new observations we divide the Nyalau Formation (Figs. 2 and 3) into the Biban Sandstone Member (Oligocene) and the Upper Nyalau Member (Early Miocene). We consider the former Kakus Member to be a separate and younger unit which is unconformably above the Nyalau Formation. Thus, it cannot be a member of the Nyalau Formation, but could be part of the Balingian or Belait Formations also unconformably above the Nyalau Formation. Because of its uncertain status we have renamed it here informally as the Kakus Unit (Figs. 2 and 3). Sediments near Kapit in the Sibu Zone (Merit-Pila synform), also previously included in the Nyalau Formation (Liechti et al., 1960), are assigned by us to a separate Merit-Pila Formation based on their different lithologies, provenance, and interpreted drainage history (Figs. 2 and 3).

4.1. Nyalau Formation

The Nyalau Formation comprises clastic sediments of Oligocene to Early Miocene age which are exposed around the towns Tatau and Bintulu (Wolfenden, 1960) (Fig. 2). Previous micropalaeontology results along with our new results, discussed in detail in section 5.1, confirm the age range. The total thickness was reported by Liechti et al. (1960) and Wolfenden (1960) as 12,000-13,000 feet (c. 3600-3900 m). It forms the thickest and laterally most extensive formation in the Tatau-Nyalau province.

4.2. Biban Sandstone Member

4.2.1. Background

The lower part of the Nyalau Formation is conformably above or interfingers with the Buan Formation (e.g. Wolfenden, 1960) and was termed the Biban Sandstone Member in the area north and south of Tatau (Liechti et al., 1960). An Early Oligocene age was assigned by W. E. Crews (in de Boer and Milroy, 1952) and by Liechti et al. (1960) based on foraminifera. The micropalaeontology is reviewed in section

5.1. Southeast of Tatau, Adams (1963) reported Lower Oligocene foraminifera from the Sarang Limestone, which he concluded forms the top of the Buan Formation or the base of the Biban Sandstone Member.

4.2.2. Field description

The Biban Sandstone Member in the research area consists predominantly of channelised sandstones and sand-dominated heterolithic deposits with intercalations of carbonaceous mudstone and siltstone, mm- to cm-thin carbonaceous layers (Fig. 4a) and some interbedded calcareous hardgrounds. Sheet-like sandstones were also observed. Heterolithic deposits show planar lamination or ripple to flaser lamination (Fig. 4b), which is locally disturbed by *Skolithos* trace fossils (Fig. 4b). The member is at least several hundred metres thick and forms prominent hills and ridges.

4.2.3. Interpretation

The Biban Sandstone Member is interpreted as multiple thick tidal channels in a tide-influenced delta. Heterolithic beds with planar and ripple lamination and non-channelised layers are typically found in a tidal environment such as tidal flats (Feldman and Demko, 2015; Quijada et al., 2016). Flaser lamination is also typically found in a tidal environment (Reineck and Wunderlich, 1968). Thin calcareous beds may represent tidal flats or lagoons. *Skolithos* trace fossils can be associated with an intertidal environment (Benton and Harper, 1997). Their low abundance suggests a stressed unfavourable environment for many organisms. The thickness of sandstone beds and high sand content of the succession suggest burrowing may have been inhibited by high input rates of clastic material accompanied by fast subsidence (Dashtgard, 2011). The intertidal interpretation is strengthened by carbonaceous material that indicates input from a vegetated floodplain. This interpretation is consistent with Liechti et al. (1960) who concluded shallow littoral to inner neritic conditions.

4.3. Upper Nyalau Member

4.3.1. Background

Liechti et al. (1960) noted that the Nyalau Formation around the town of Similajau (and the Nyalau River) north of Bintulu cannot be subdivided into members or clearly distinguished from the lower parts, and assigned exposures in this area simply to the Nyalau Formation. We use the term Upper Nyalau Member for the successions in this area to distinguish them from the underlying Biban Sandstone Member and the overlying Kakus Unit. In future the section along the newly built road from Bintulu to Similajau, crossing the Sungai Similajau, could serve as type section for what could then be called a Similajau Member. A Late Oligocene ($Te_{1\text{-}4}$) to Early Miocene (Te_5) age was interpreted by Liechti et al. (1960) and Kho (1968) based on foraminifera. We identified an Early Miocene foraminifera assemblage (Te_5 to Tf; N4 to N6, see section 5.1) that supports the previous age interpretation.

4.3.2. Field description

The succession north of Bintulu includes cm- to m-thick sandstone beds interbedded with rippled sandstone, heterolithic deposits and rarely mudstones (Fig. 4c). Towards the north, the thickness and abundance of the sandstone beds gradually decreases and the proportion of mudstone, heterolithic deposits and calcareous beds increases (Fig. 4d). Sandstone beds are massive, horizontal laminated or channelised with trough cross-bedding (Fig. 4c and e). Heterolithic deposits show crudely developed ripples that are predominantly symmetrical wave ripples. Bioturbation is moderate and includes *Cruziana* (Fig. 4f), *Ophiomorpha* and *Skolithos*. Calcareous beds are up to 8 cm thick and contained fragments of coralline algae (Fig. 4g) and larger benthic foraminifera. In the area north of Similajau shale and mudstone are the dominant lithologies and it is not possible to distinguish the Setap Shale Formation and the shale-dominated Nyalau Formation.

4.3.3. Interpretation

The heterolithic beds and wave ripple lamination indicate fluctuating water energy levels and weak currents with wave oscillations dominant, which are typical of tide-influenced environments (Vakarelov et al., 2012). The thick mudstone layers suggest a delta plain, tidal flats or coastal floodplain. The thick channelised cross-bedded sandstone beds are interpreted as tidal channels that cut into and migrate over the delta plain, and isolated sand bodies represent tidal sand bars (Dalrymple and Choi, 2007 and references therein). Calcareous layers with bioclasts could represent tidal flats or lagoons, but could alternatively be input from a nearby reef or forereef at greater water depths. The *Cruziana* ichnofossils also indicate a shelf environment below the fair weather wave base (Benton and Harper, 1997). The depositional environment ranges from delta plain to possible mid shelf consistent with the fluvial littoral to inner neritic conditions interpreted by Kho (1968).

4.4. Kakus Unit

4.4.1. Background

The informal term Kakus Unit is used in this study for sediments assigned to the Kakus Member by Liechti et al. (1960) and interpreted by them as the uppermost part of the Nyalau Formation. Previously Kirk (1957) had used the term Kakus Formation. The lower boundary of the Kakus Member was reported to be a diachronous facies boundary based on mapping (Kirk, 1957; Liechti et al., 1960), but difficulties in delimiting the Kakus deposits (see Liechti et al., 1960, pages 123-126) hinder a clear identification of the boundaries. The name is derived from the remote and inaccessible Kakus River area (Fig. 2), but no type section was assigned. We studied the succession in the Bala Anticline and Segan Syncline near Bintulu (Fig. 2), in another area previously mapped as Kakus Member (Liechti et al., 1960). An Early Miocene age was reported by Hassan et al. (2013) on the basis of palynological analysis of deposits in the area of Bintulu that include the Kakus Unit. Liechti et al. (1960) suggested an age of possible Te_5 to Tf (Miocene), but no age determining microfossils were found.. As discussed below (section 8.2) the sediments mapped as Kakus Member near Bintulu have a different provenance character to those of the Nyalau Formation. We consider them to rest unconformably on the Nyalau Formation, and therefore exclude them as a member of the Nyalau Formation. However, detailed mapping and more research is needed to reexamine the stratigraphic position of other exposures that were previously mapped as Kakus Member to consider their status (for example, a separate Kakus Formation or a member of another formation such as the Belait or Balingian Formations).

4.4.2. Field description

The succession in the Bintulu area is composed of heterolithic deposits, cm- to m-thick sandstone beds, thick (from several cm to m) carbonaceous mudstones, and thin (cm) coal seams (Fig. 5a and b). Sandstones and heterolithic beds show crudely developed cross-bedding (planar and trough) and ripples (Figs. 5c and d). Ripples are usually asymmetrical, but some symmetrical wave ripples were also observed with ripple tops composed of mud (Fig. 5c). Crests of cross-beds are formed by mud drapes (Fig. 5d). Sandstone-dominated and heterolithic deposits show moderate bioturbation by *Skolithos* and *Ophiomorpha* (Figs. 5d and e). There are no calcareous layers, unlike the Biban Sandstone and Upper Nyalau Members.

4.4.3. Interpretation

The Kakus Unit indicates very similar environments to those of the Nyalau Formation, which are tidal flats, tidal channels and floodplain. Mud drapes on cross-beds are typical of tidal sand waves (Allen, 1982). Observed ripples indicate uni- and bi-directional flow regimes, suggesting a mixed environment of wave- and current-flows, the latter representing the influence of tides (Vakarelov et al., 2012). Carbonaceous mudstones and coal seams indicate abundant input from vegetated floodplain areas. The ichnofacies indicates an intertidal environment (Benton and Harper, 1997) and the abundance of bioturbation suggests episodes with limited clastic input. The absence of calcareous material suggests no nearby reefs. We infer water depths for the Kakus Unit to have been shallower than the Nyalau Formation, like Liechti et al. (1960), possibly including only delta front and delta plain environments with little lateral facies variation. Liechti et al. (1960) suggested paralic conditions and Hassan et al. (2013) interpreted a tide-dominated to coastal floodplain environment.

4.5. Merit-Pila Formation

4.5.1. Background

The term Merit-Pila Formation is introduced in this study for sediments of the Merit-Pila synform near the town of Kapit in the Sibu Zone (Fig. 2). These were originally assigned to the Long Formation by de Boer and Milroy (1952) and to the Pila Coal Formation by Kirk (1957). Liechti et al. (1960) grouped them with other exposures of similar rocks across the Sibu Zone as the “Nyalau Formation in the Rajang Hinterland” in contrast to the “Nyalau Formation in the Miri Zone”. A Late Oligocene to Miocene age was assumed by Kirk (1957) and Liechti et al. (1960). Jordi and Bowen (1956) reported Upper Oligocene ($Te_{1\text{-}4}$) larger foraminifera from sediments at Batu Bora, potentially equivalents of the Merit-Pila Formation. Abdullah (2001) suggested an Early Miocene age based on coal constituents in the Merit-Pila deposits.

As this study identified differences in petrography, provenance and depositional environment from the Nyalau Formation in the Miri Zone we propose this new term. Detailed mapping by Liaw (1987) suggests a thickness of c. 600 to 1000 m for the Merit-Pila Formation. Other exposures assigned to the Nyalau Formation in the Sibu Zone e.g. at the Hose Mountains or at Batu Bora, which are potential equivalents of the Merit-Pila Formation are reported (Jordi and Bowen, 1956; Liechti et al., 1960) to be unconformably above the Rajang Group in the Hose Mountains area and in the Kaluan and Linau Rivers areas (Fig. 2).

4.5.2. Field description

The succession is composed of conglomerates (Fig. 6a), channelised (Fig. 6b) or sheet-like coarse-grained sandstones, rippled sandstones with asymmetrical current ripples (Fig. 6a), fine sandstone-mudstone alternations, carbonaceous mudstones, and coal seams. Conglomerates are abundant at the base of the formation and are composed of sandstone, quartz, chert, coal and mudstone clasts

(Figs. 6c and d) and have typically an erosive base (Fig. 6d). The sandstone clasts are usually dark coloured and resemble the nearby Belaga Formation (Fig. 6c). Trough cross-bedded sandstone with thin conglomerate bands form channels that truncate underlying cross-beds (Fig. 6e). Planar cross-bedding and climbing ripples were also observed (Fig. 6f). Usually carbonaceous mud forms the crests of the cross-beds and ripple tops (Fig. 6f). Centimetre-thick coal seams or coal fragments are present within the sandstones (Fig. 6g). Higher up in the formation fine-grained sediments are more common. Mudstone deposits of about 3 m thickness are dissected by channel sandstones from cm to a few m thick (Fig. 6h). The uppermost part of the successions is formed by thinly-bedded sandstone-mudstone alternations. Although the contact is not exposed the formation is interpreted to rest unconformably on the Belaga Formation which is moderately to steeply dipping, whereas the Merit-Pila Formation dips at a low angle towards the NW or SE.

4.5.3. Interpretation

The Merit-Pila Formation consists mainly of fluvial deposits and includes clasts of the underlying Belaga Formation. Conglomerates are coarse channel fills or lag deposits (Miall, 1985; Labourdette and Jones, 2007). Sandstones were channels or bars in a fluvial environment. Sheet-like geometry is probably related to deposition of hyperconcentrated, fluidal and plastic stream flows in a braided system (Martin and Turner, 1998) recording sheet-flood events or are a product of amalgamation of complex, multi-storey sandstone beds (Williams and Hillier, 2004). Current asymmetrical ripples indicate unidirectional flow and climbing ripples suggest high sediment influx. Fine laminated sands suggest overbank or flood deposits (Miall, 1985). Carbonaceous mudstones and coals indicate a swamp or coastal floodplain environment (Miall, 1985; McCabe, 1987).

4.6. Setap Shale, Tangap and Sibuti Formations

4.6.1. Background

The term Setap Shale Formation was introduced by Liechti et al. (1960) for shale-dominated deposits in the northern part of the Miri Zone where there is a monotonous succession of shale, c. 700 – 4700 m thick, which is interbedded with thin sandstone beds and a few limestone lenses (Liechti et al., 1960; Kho, 1968). Locally, the shales have been assigned to other formations (e.g. Sibuti Formation, Suai Formation, Tangap Formation, Tubau Formation) based on minor lithological differences (Liechti et al., 1960; Heng, 1992; Banda and Honza, 1997; Lee et al., 2004). The Setap Shale Formation is of Late Oligocene to Early Miocene age (Haile, 1962; Sandal, 1996) and is unconformably above the Rajang Group (Liechti et al., 1960). It is interpreted as the holomarine equivalent of the Nyalau Formation (Hutchison, 2005).

The Tubau Formation comprises shales, calcareous shales and marls interbedded with thin beds of sandy or silty shales. It was assumed to be unconformable above the Belaga Formation (Liechti et al., 1960) and may be the oldest equivalent of the Setap Shale Formation or underlie it (Fig. 3). Its age was reported age as Late Oligocene to Early Miocene (Liechti et al., 1960). No exposures of the Tubau Formation were analysed in this study.

The Tangap Formation is composed predominantly of calcareous shales with marls, sandstones and limestones (Haile, 1962). It is reported to interfinger with the Nyalau Formation (Liechti et al., 1960; Haile, 1962). The Subis Limestone is a member of this formation (Haile, 1962) and forms the limestone cliffs at Gunung Subis. Haile (1962) and Mihaljevic et al. (2014) reported Oligocene to Lower Miocene foraminifera.

The Sibuti Formation consists of alternations of calcareous shales and mudstones with minor siltstones that overlie the Subis Limestone and the formation is an equivalent of the upper part of the Setap Shale Formation (Banda and Honza, 1997; Hutchison, 2005; Kessler and Jong, 2015). Liechti et al. (1960) mapped exposures of the Sibuti Formation as the Setap Shale Formation, but according to Lee et al. (2004) the Sibuti Formation can be distinguished by a higher fossil content, marl lenses, and abundant limestone beds. It is assumed to be Late Oligocene to Early Miocene (Haile, 1962; Banda and Honza, 1997; Simmons et al., 1999).

4.6.2. Field description

The Setap Shale Formation and its equivalents in the research area are composed of dark coloured shales and mudstones (Fig. 7a) interbedded with cm-thin sandstones and siltstones, and may include carbonaceous, calcareous or marly lithologies (Fig. 7b). Thin siltstone to sandstone beds commonly show gentle folding or slumping. Marls and thin limestones are common in the Tangap Formation and are also present in the Sibuti Formation, but are subordinate in the Setap Shale Formation. The Subis Limestone forms an isolated limestone platform (Fig. 7c) within the Tangap Formation. Samples analysed in this study yielded abundant benthic foraminifera, algae and coral fragments. Calcareous layers of the Setap Shale Formation collected in this study yielded planktonic foraminifera described below.

While most of the Setap Shale Formation dips at low angles towards the north, the Sibuti Formation and parts of the Setap Shale Formation in the north are locally folded, resulting in exposures of sub-horizontal to steeply dipping beds. Channels filled with cm-thin sandstones or siltstones cut into the shale (Fig. 7d). Ten kilometres south of Beluru (Fig. 2; location Si-01) the Sibuti Formation, which consists of grey coloured sandstone-siltstone alternations, overlies weathered loose mudstones of the Setap Shale Formation with a distinct disconformity (Fig. 7e).

4.6.3. Interpretation

The Setap Shale, Sibuti and Tangap Formations indicate an open marine shelf environment with fine clastic input. Carbonaceous material indicates wash-in from coastal floodplains, while marls indicate input from nearby reefs or tidal flats. Slumps record syn-sedimentary deformation on a paleoslope (McGilvery and Cook, 2003; Meiburg and Kneller, 2010). The Sibuti Formation with its higher content of calcareous beds represents inner shelf deposits, and channels observed within the formation are interpreted as distal tidal channels or as prodelta deposits (Allen and Chambers, 1998). The Tangap Formation with the Subis Limestone forms a reef complex. Liechti et al. (1960) and Kho (1968) interpreted a shallow littoral to inner neritic depositional environment for the formations.

5. Micropalaeontology

In the biostratigraphic study of the thin sections, we primarily use the planktonic foraminiferal zones which were defined by BouDagher-Fadel (2015) and calibrated against the biostratigraphical time scale and radioisotopes (as defined by Gradstein et al., 2012 and revised by Cohen et al., 2017). The planktonic foraminiferal zonal scheme of BouDagher-Fadel (2015) is also correlated with the larger benthic foraminiferal 'letter stages' of the Far East, as defined by BouDagher-Fadel and Banner (1999) and later revised by BouDagher-Fadel (2018).

5.1. Nyalau Formation

We did not find foraminifera in our samples from the Biban Sandstone Member. Wolfenden (1960) however, reported larger foraminifera interpreted to indicate an Oligocene age (Tcd to Te_{1-4}). Recorded Lower Oligocene foraminifera included *Nummulites* cf. *absurda* (Doornink), *Nummulites divina* (Doornink), *Nummulites* cf. *intermedius* (d'Archiac), *Nummulites* spp. (reticulate and striate) and *Operculina* sp., and Upper Oligocene foraminifera included *Cycloclypeus* sp?, *Eulepidina* sp., *Heterostegina* sp?, *Lepidocyclina (Nephrolepidina)* sp., *Lepidocyclina* sp., *Operculina* cf. *pyramidum* (Ehrenberg), *Operculina* sp., operculinids and rotalid (Wolfenden, 1960), however, *O. pyramidum* is an upper Eocene form first recorded from the Eocene of Egypt. Those recorded from the Oligocene of Borneo belong to a different species/genus (Cole, 1957, Abd El-Gaied et al., 2019) and the rest of the listed upper Oligocene larger benthic foraminifera occur in the Early Miocene too (see BouDagher-Fadel, 2018). Kho (1968) reported *Heterostegina* cf. *borneensis* van der Vlerk, *Lepidocyclina* (*Eulepidina*) sp., *Lepidocyclina* (*Nephrolepidina*) spp. and *Cyclolypeus* cf. *eidae* Tan indicating a Late Oligocene age, however, *H.* (*V.*) *borneensis* and *C. eidae* are both widespread in the Indo-Pacific Late Oligocene and Early Miocene (see Tan Sin Hok, 1932; Özcan and Less, 2009; BouDagher-Fadel and Price, 2013, 2014; BouDagher-Fadel, 2018) and therefore this assemblage is indicative of both Late Oligocene and Early Miocene.

Three thin sections were analysed biostratigraphically from the Upper Nyalau Member in this study. Sample Ny-04, is a grainstone with some quartz and larger benthic foraminifera. The sample include fragments of *Eulepidina* spp., *Lepidocyclina oneatensis, Operculina* sp., *Heterostegina* (*Vlerkina*) *borneensis*, *Eulepidina badjirraensis*, *Lepidocyclina stillafera* (Fig. 8a), and fragments of rodophyte spp. *Heterostegina* (*Vlerkina*) *borneensis* has been recorded by some authors as restricted to the Oligocene (Chattian, P21b-P22; Te_{1-4}, Renema, 2007). The type species of *Heterostegina* (*Vlerkina*), *H.* (*V.*) *borneensis* van der Vlerk was initially described from the Early Miocene, N4-N6, in direct association with *Miogypsina, Miogypsinoides, Eulepidina, Spiroclypeus,* and the planktonic foraminifera *Globigerinoides quadrilobatus, Catapsydrax dissimilis, Globoquadrina dehiscens* (Eames et al., 1962). The description was later amended by Banner and Hodgkinson (1991), who described the original types from the Late Oligocene of Borneo. However, BouDagher-Fadel and Banner (1999) noted that although "*Heterostegina* (*Vlerkina*) *borneensis* van der Vlerk may be restricted in Melanesia to the lower part of the Te interval, but evidence from Borneo has shown that it ranges throughout the Te interval in the eastern region as a whole". This was confirmed later by BouDagher-Fadel and Price (2013, Fig. A6q) who figured *H.* (V.) *borneensis* in the same assemblage as *Lepidosemicyclina banneri* BouDagher-Fadel and Price, *Lepidosemicyclina* being a Middle Miocene form (Renema, 2007, BouDagher-Fadel and Price, 2013, BouDagher-Fadel, 2018). *H.* (*V.*) *borneensis* has also been recorded from the Tf_1 stage or early Middle Miocene age Calcarenite Member of the Pamutuan Formation, West Java, Indonesia in association with *Katacycloclypeus annulatus* (Isnaniawardhani, 2018). Elsewhere *H. (V.) borneensis* has been recorded from the Early Miocene of the Gebel Shabrawet area, northeastern desert Egypt (Abdelghany, 2002) and from the Te_5, Aquitanian, in the Solomon Islands, SW Pacific (Eames et al., 1962). In the studied sample, *H. (V.) borneensis* is associated with *Lepidocyclina stillafera* Scheffen (Fig. 8a), recorded previously from the Tf_1 "letter stage" of late Burdigalian to Langhian age, of eastern Borneo, Kalimantan and the Kalumpang Formation in Tawau, Sabah (BouDagher-Fadel and Lokier, 2005; Asis and Jasin, 2015) and *Eulepidina badjirraensis*, an Early Miocene form (see Chaproniere, 1975, 1984; BouDagher-Fadel and Price, 2010) indicating an Early Miocene age (N5b-N6).

Sample Ny-06a is a packstone of larger benthic foraminifera including assemblages of *Lepidocyclina* (*Nephrolepidina*) *sumatrensis, Spiroclypeus* sp., *Austrotrillina asmariensis (*Fig. 8b)*, Miogypsinoides dehaarti, Miogypsina tani* (Fig. 9a). *A. asmariensis* has a Tethyan stratigraphic range from Late Oligocene (Chattian) to Early Miocene (Burdigalian). It has been found commonly in the Burdigalian of the Asmari Formation, in South West Iran, Zagros Basin (Roozbahani, 2011) and the Tf_1 (Langhian) of Kali Sambi in the Gunung Sewu area of South Central Java (BouDagher-Fadel and Lokier, 2005). The occurrence of *A. asmariensis* in association with *Miogypsinoides dehaarti* and *Miogypsina tani* indicates an Early Miocene age, Late Aquitanian - Burdigalian, N5a-N6, 21.0-17.2 Ma.

Sample Ny-6b is a packstone of larger benthic foraminifera including assemblages of *Lepidocyclina (Nephrolepidina) sumatrensis* (Fig. 8c)*, Spiroclypeus* sp., *Heterostegina* (*Vlerkina*) *borneensis, Lepidocyclina stratifera, Spiroclypeus tidoenganensis* (Fig. 8d)*, Miogypsinoides bantamensis, Miogypsina kotoi* (Fig. 9b)*.* The latter has been described from the Early Miocene of Borneo (see BouDagher-Fadel and Price, 2013). *Miogypsinoides bantamensis* has been recorded from the Oligocene and Early Miocene of the Mediterranean (BouDagher-Fadel and Price, 2013), the latest Oligocene and Early Miocene (Raju, 1974; Drooger, 1993), the Miocene of Japan (Matsumaru, 2012), the Miocene of the Indo-Pacific (BouDagher-Fadel, 2018). In this sample the occurrence of *Miogypsine kotoi* and *Miogypsinoides bantamensis* indicates an Early Miocene age, Aquitanian – Early Burdigalian, N4-N5b, 23-18 Ma.

Commented [T1]: N5a only until 20.2, N5b until 18 Ma

Commented [BM2R1]: Yes you are right. This is a mistake N5b as both bantamensis and Vlerkina all ranges till N5b

This age interpretation is in accordance with Haile (1962) and the Sarawak Shell Oilfields Limited age determination (in Kho, 1968) who concluded a Te_5 to possible Tf (Early to ?Middle Miocene) age of the Nyalau Formation around Bintulu based on the occurrence of *Miogypsinoides dehaartii* van der Vlerk and *Miogypsina* s.s.

5.2. Subis Limestone

Two samples from the Subis Limestone were analysed in this study. Sample Sub-01a is a wackestone of larger benthic foraminifera including assemblages of *Spiroclypeus* sp., *Planorbulinella solida*, *Eulepidina* sp., *Lepidocyclina* sp., *Miogypsinodella primitiva* (Fig. 8e), *Amphisorus martini* (Fig. 8f), *Miogypsina intermedia* (Fig. 9c), miliolid spp., echinoid spp., rodophyte spp. The presence of *Miogypsinodella primitiva* and *M. intermedia* indicate a Burdigalian age, N5b-N6, 20.4-17.2 Ma (Raju, 1974; Drooger, 1993; Ferrandini et al., 2010; BouDagher-Fadel and Price, 2013; BouDagher-Fadel, 2018).

Commented [T3]: N5b from 20.4; N5 from 21

Commented [BM4R3]: Yes corrected

Sample Sub-01b is a wackestone of larger benthic foraminifera including assemblages of *Spiroclypeus* sp., *Eulepidina* sp., *Lepidocyclina* sp., small miliolids, *Textularia* spp., *Austrotrillina asmariensis*, rodophyte spp. The presence of *A. asmariensis* indicates a Late Aquitanian – Burdigalian age, N5-N8a, 21-15.4 Ma (BouDagher-Fadel, 2018).

5.3. Setap Shale Formation

Two samples of the Setap Shale Formation have been analysed for biostratigraphy in this study. Samples Set-01a/b are wackestones with planktonic foraminifera. The presence of *Catapsydrax dissimilis* (Fig. 8g), *Paragloborotalia continuosa* (Fig. 8h), *Globigerinoides quadrilobatus* (Fig. 8i) indicates an Early Miocene age, N4-N6, 23-17.2 Ma (see BouDagher-Fadel, 2015).

Kho (1968) reported results from Sarawak Shell Oilfields Limited from the Setap Shale Formation samples north of the Bala Anticline (Sibiu Valley) that included a Te$_{1\text{-}4}$ fauna (Late Oligocene) with *Lepidocyclina* sp., *Operculina* sp., *Spiroclypeus* sp., *Amphistegina* sp., *Cycloclypeus* sp., and a Te$_5$ (Early Miocene) with *Operculina* sp., *Miogypsinoides dehaartii*, *Anomalina* sp., *Asterigerina* sp., *Cyclammina* sp., *Flosculinella* sp., *Operculina* spp., *Quinquelocullina* sp., *Rotalia* spp., *Sigmoidella* sp., *Sigmoilina* sp. and *Textularia* sp.

6. Light mineral assemblages

Analysed samples from the Nyalau Formation, Kakus Unit and Merit-Pila Formation have relatively low amounts of matrix (<14 %) (Tab. 2) and are all classed as arenites. They comprise generally quartz-rich sandstones (50 to 77 % framework grains) with feldspars (5 to 20 % framework grains) and various lithic fragments (18 to 39 % framework grains) (Tab. 2). The Merit-Pila and Kakus Unit samples are sublitharenites, and those from the Biban Sandstone and Upper Nyalau Members are predominantly lithic arenites (Fig. 10), reflecting their higher content of lithic fragments (average of 28.3 %). Grains are dominated by monocrystalline quartz, with additional abundant polycrystalline quartz, feldspar, and sedimentary and metamorphic lithic fragments. Sedimentary lithic fragments consist of mudstone, siltstone and rare sandstone clasts; all of them have a slight metamorphic overprint. Metamorphic lithic fragments are predominantly composed of quartz-mica schist clasts. Subordinate are chert, volcanic lithic fragments (mafic and felsic) and volcanic quartz. Grains are usually angular to subrounded and indicate a low textural maturity.

The moderate quartz and high lithic fragment contents are in accordance with a recycled orogen character (Fig. 10). Further, a transitional and quartzose recycled orogen character can be assigned, based on the contents of polycrystalline quartz and chert (Fig. 10).

7. Heavy mineral assemblages

Seven samples were analysed for heavy minerals and compared to published data from the underlying and overlying successions. Count numbers of analysed samples can be found in Supplementary Tab. 2. Heavy mineral assemblages are dominated by ultra-stable zircon, tourmaline and TiO_2 polymorphs, reflected in the very high ZTR values of 73 to 91 (Tab. 3) that show the percentage of the three ultra-stable minerals from the total number of translucent heavy minerals (Hubert, 1962). In most samples TiO_2 polymorphs are the main heavy mineral representing 30 to 50 % of the translucent assemblage. They are often heavily corroded and appear opaque or near-opaque in many of the samples, thus it is very difficult to identify them optically or to distinguish between different TiO_2 polymorphs. Rutile is the dominant polymorph and some brookite was optically identified. EDS analysis shows some TiO_2 polymorphs have significant amounts of Nb and could be classed as niobian rutile. Zircon is the second-most abundant heavy mineral with 15 to 43 % of the translucent assemblage. The Nyalau Formation samples (Biban Sandstone and Upper Nyalau Members) have the lowest zircon abundances of about 15 to 20 % (Tab. 3). Tourmaline is the third-most abundant heavy mineral with 7 to 29 % of the translucent assemblage (Tab. 3). Brown amphibole is a trace heavy mineral in most samples and is often heavily corroded and weathered.

Samples from the Biban Sandstone Member and the Upper Nyalau Member are characterised by a high ratio of TiO_2 polymorphs to zircon (Fig. 11), reflected in the high RZi (TiO_2 group-zircon index; Morton and Hallsworth, 1994) between 70 and 80 (Tab. 3), which means TiO_2 polymorphs are approximately three times more abundant than zircon. In contrast, the Kakus Unit sample and the Merit-Pila Formation samples have more abundant zircon (Fig. 11) and a lower RZi ratio of below 50. The ZTi ratio (zircon-tourmaline ratio; e.g. Mange and White, 2007) is low for the Biban Member and Upper Nyalau Member with values of 34 to maximal 60, while samples from the Kakus Unit and the Merit-Pila Formation have high ratios of 69 to 85 (Tab. 3).

Other translucent heavy minerals identified include garnet (trace to 9 %), apatite (trace to 7 %), monazite (1 to 4 %), xenotime (trace), chrome spinel (2 to 5 %) and APS (aluminium-phosphate-sulphate) group minerals (trace to 9 %) (Tab. 3; Fig. 11). Scheelite, baryte, sphalerite and jarosite are present in one or two samples (Tab. 3). Most notable is the amount of garnet (9 %) and apatite (7 %) in sample Ny-03, in contrast to all other samples in which they are only trace components (Tab. 3; Fig. 11). There are two possible explanations for this: garnet and especially apatite are susceptible to acid dissolution and might have been removed during acid leaching of the other samples, rather than indicating a source change, or Ny-03 was less affected by acid waters. Generally, the Upper Nyalau Member samples have more abundant garnet and apatite than the Biban Sandstone Member samples.

Chlorite and other undifferentiated mica are common in the samples (up to 10 % for chlorite and 36 % for mica from the total heavy mineral assemblage) and opaque minerals include ilmenite, pseudorutile, iron oxides, pyrite and chalcopyrite (Tab. 3). Ilmenite in the samples often contains Al and P that indicates alteration processes (Dill et al., 2007), and there is abundant pseudorutile (trace up to 11 % of the total heavy mineral assemblage), which forms the most abundant opaque heavy mineral phase (Tab. 3). Additionally, some ilmenorutile (Nb-bearing ilmenite) was found in most of the samples. The Kakus Unit sample TB50 and the Merit-Pila Formation samples have very similar heavy mineral assemblages, differing only in the low amount of APS minerals in TB50.

8. U-Pb geochronology

8.1. Nyalau Formation in the Miri Zone (Biban Sandstone and Upper Nyalau Members)

U-Pb dating of detrital zircons was carried out on samples from the Nyalau Formation in the Miri Zone. Samples TB52 and TB51 were from the lower part (Biban Sandstone Member) and samples Ny-03 and Ny-05 were from the upper part in the Similajau area. The four samples have similar detrital zircon age populations. A total of 131 concordant U-Pb ages were obtained from 134 zircon grains of sample TB52, 129 concordant ages from 131 zircon grains of TB51, 121 concordant ages from 123 zircon grains of Ny-03, and 113 concordant ages from 122 zircon grains of sample Ny-05.

The four samples are all dominated by Phanerozoic ages, but also have a significant number of Precambrian ages (Fig. 12). Characteristic is a dominant Permian-Triassic population in the Phanerozoic, generally with peaks around 230 to 260 Ma (around the P-T boundary) and 210 to 230 Ma in the Late Triassic. Cretaceous zircons form the second largest population and range from the Early to Late Cretaceous with peaks at 100 to 120 Ma and 70 to 80 Ma. Samples from the Upper Nyalau Member (Ny-03, Ny-05) have a more pronounced Cretaceous peak than the samples from the lower part (Biban Sandstone Member). There is a small number of Oligocene to Early Miocene zircons that indicate some magmatic activity around the time of deposition. There are minor Paleozoic and Proterozoic age populations. Precambrian ages peak at c. 1.8 Ga and range into the Archean with a smaller peak at c. 2.5 Ga. The oldest grains are 3267 ± 7 Ma in sample Ny-03 and 3185 ± 10 Ma in sample TB52. The youngest grains were found in sample Ny-05 with 19.1 ± 0.4 Ma, in sample Ny-03 with 31.1 ± 0.4 Ma and in sample TB51 with 25.2 ± 0.5 Ma.

8.2. Kakus Unit (Bala Anticline - Segan Syncline)

The Bala Anticline–Segan Syncline deposits were sampled from south of Bintulu. The zircon populations of sample TB50 differ from samples analysed from the Nyalau Formation in their abundance of Cretaceous detrital zircons. A total of 119 concordant U-Pb ages were obtained from 123 zircon grains (Fig. 12). Zircon populations consist of 93 Phanerozoic, 20 Proterozoic and 6 Archean ages and are dominated by Cretaceous ages that form c. 40 % of all analysed zircons. In contrast, Nyalau Formation samples have only about <20 % Cretaceous zircons. The Cretaceous population in TB50 ranges from c. 70 to 145 Ma with major peaks between c. 100 to 120 Ma and at c. 140 Ma. There are additional minor populations in the Jurassic, Triassic and Late Permian. A few Carboniferous, Devonian, Silurian, Devonian and Cambrian ages make up the Paleozoic fraction. The Precambrian zircons form a prominent peak at c. 1.8 Ga, with a few scattered ages between c. 0.8 to 1.0 Ga and c. 2.4 to 2.9 Ga. The oldest age recorded in sample TB50 is 2892 ± 8 Ma and the youngest is 71 ± 1 Ma.

8.3. Merit-Pila Formation

The Merit-Pila Formation was sampled from the Merit-Pila synform (TB244a and TB243) north of the town Kapit along the Rajang River in the Sibu Zone (Fig. 2). The two samples have very similar zircon populations. A total of 138 concordant U-Pb ages were obtained from 137 zircon grains of sample TB244a and 112 concordant U-Pb ages were obtained from 128 zircon grains of sample TB243 (Fig. 13).

The samples from the Merit-Pila Formation have a large number of Cretaceous zircons, which peak between 90 and 130 Ma. In contrast to the Kakus Unit sample they have a higher number of Precambrian and Permian-Triassic zircons. Permian-Triassic zircons are abundant and peak around c. 240 to 260 Ma. There are a number of Late Jurassic ages at c. 150 to 160 Ma, and an Ordovician-Silurian peak around c. 440 to 450 Ma. Paleoproterozoic ages at c. 1.8 Ga are the most abundant Precambrian population. Scattered ages at c. 800 to 900 Ma and 2.5 Ga complement the Precambrian population. The oldest age is recorded in sample TB243 with 2786 ± 38 Ma and the youngest is 81 ± 1 Ma in TB244a.

9. Discussion

9.1. Age of deposition

We use the new biostratigraphic data and previous literature to clarify ages of deposition of different members and formations. The oldest part of the Nyalau Formation (Biban Sandstone Member) was deposited in the late Early Oligocene based on foraminifera data by Wolfenden (1960), above the Lower Oligocene fluvial-deltaic-tidal Tatau and holomarine Buan Formations. The Biban Sandstone Member records a significant increase in clastic material and subsidence of the basin to deposit the thick sand-dominated lower part of the Nyalau Formation. The Upper Nyalau Member is characterised by heterolithics and sandstone beds that interfinger with thick mudstones and siltstones and was deposited in the Early Miocene based on the new foraminifera data.

Based on significant provenance differences identified in this study which are discussed further below, we consider the Kakus deposits to be separate from the Nyalau Formation and, as explained above, use the term Kakus Unit for them. The Kakus Unit was deposited in the latest Early Miocene or the earliest Middle Miocene, inferred from the age of the overlying or contemporaneous Balingian Formation whose deposition began in the latest Early Miocene or earliest Middle Miocene (Nugraheni et al., 2014; Hennig-Breitfeld et al., 2019).

There are no biostratigraphic data available for the Merit-Pila Formation in the Sibu Zone. These outliers have been assumed to be Miocene (Kirk, 1957; Liechti et al., 1960) and some potential equivalents along the upper Rajang River (Batu Bora) are reported to be Late Oligocene (Liechti et al., 1960). The Merit-Pila Formation has a dominantly fluvial to alluvial fan character, but Konzalová (2005) and Osvald and Sykorova (2006) reported coastal plain and mangrove swamp indicators, suggesting proximity to the coast.

The Setap Shale Formation in onshore Borneo was deposited between the Oligocene and Early Miocene, at the same time as the Nyalau Formation, and in particular its upper part, based on the samples analysed in this study. The Subis Limestone samples have an Aquitanian to Burdigalian age range, consistent with reports by Roohi (1998) and Mihaljevic et al. (2014) who recorded Aquitanian benthic foraminifera from the lower parts of the limestone. Planktonic foraminifera reported by Simmons et al. (1999) for the Sibuti Formation indicate an Early Miocene to late Early Miocene age similar to the samples of the Setap Shale Formation of this study.

9.2. Sediment sources

All studied samples from the Nyalau Formation, Merit-Pila Formation and Kakus Unit are compositionally moderately mature and texturally immature quartz-rich sedimentary rocks, which indicate first-cycle or only moderately recycled clastic deposits. Interpretation of provenance based on light minerals can be difficult in humid climate conditions, as intensive feldspar dissolution and breakdown of unstable lithic fragments occurs (e.g. Suttner et al., 1981; Sevastjanova et al., 2012; van Hattum et al., 2013). The Nyalau Formation samples have generally higher contents of lithic fragments (especially more metamorphic and volcanic lithic fragments) and feldspar, than samples from the Merit-Pila Formation and Kakus Unit (Fig. 10, Tab. 2). We interpret this to reflect differences in sources which is supported by the heavy mineral assemblages and the U-Pb detrital zircon geochronology. Feldspar and volcanic and metamorphic lithic fragments indicate input from igneous and metamorphic basement rocks.

Heavy mineral assemblages are dominated by ultra-stable minerals, dominated by zircon, tourmaline and TiO_2 polymorphs (mainly rutile). Subordinate APS group minerals related to alteration of phosphorite deposits or weathering of tropical soils (Dill, 2001), and pseudorutile related to leaching of ilmenite placers or beach sands (Bailey et al., 1956; Mücke and Bhadra Chaudhuri, 1991; Mange and White, 2007) indicate alteration processes. Apatite and garnet dissolution may also have taken place, considering their absence in most samples. Variations in abundance of zircon, TiO_2 polymorphs and tourmaline support similar differences between formations to those indicated by light minerals. The Nyalau Formation samples with high RZi and low ZTi values can be distinguished from the Merit-Pila Formation and the Kakus Unit which have more abundant zircon and significantly less tourmaline (Fig. 11). The ZTi and RZi differences between the Nyalau and the Merit-Pila Formation/Kakus Unit indicate different sources. The slightly higher contents of garnet, apatite, amphibole and ilmenite in the Nyalau Formation samples suggest greater input from igneous or metamorphic basement, supporting inferences based on light minerals. Chrome spinel present in all samples indicates minor input from an ultramafic source.

The clearest provenance indicator is based on detrital zircon geochronology. The Nyalau Formation samples are dominated by Permian-Triassic zircons, with minor Cretaceous and Precambrian (c. 1.8 Ga) age peaks (Fig. 12). The Malay-Thai peninsula (Sevastjanova et al., 2011; Searle et al., 2012) is a potential source for Permian-Triassic, Precambrian and minor Cretaceous detrital zircons. Cretaceous zircons could also be derived directly, or indirectly from recycled sediments, from southern Vietnam (Nguyen, T.T.B. et al., 2004; Shellnutt et al., 2013; Fyhn et al., 2016; Hennig et al., 2018; Nguyen, H.H. et al., 2018). The West Borneo province has also similar age populations (Breitfeld et al., 2017; Hennig et al., 2017a) which could account for Cretaceous zircons and Permian-Triassic zircons. Cretaceous zircons are slightly more dominant in the Upper Nyalau Member (Fig. 12), suggesting increased input from Borneo (source for Cretaceous zircons) related to uplift at the time of deposition of the upper parts of the Nyalau Formation.

In contrast, the contemporaneous Merit-Pila Formation is characterised by a much larger Cretaceous age peak (Fig. 13), suggesting a greater input from a Borneo source. The broad Cretaceous peak corresponds to Schwaner magmatism that ranged from c. 80 Ma to 130 Ma (Davies et al., 2014; Hennig et al., 2017a), or sediments derived from it (e.g. Kuching Supergroup, Rajang Group). Recycled clasts of Belaga Formation observed in the field support this interpretation. However, Permian-Triassic zircons indicate a Malay-Thai or West Borneo contribution, most likely by recycling sediments of the Kuching and Sibu zones . Ordovician-Silurian, Neoproterozoic, c. 1.8 Ga and c. 2.5 Ga zircons are all minor constituents of Mesozoic and Paleogene sedimentary rocks from Borneo (e.g. Pedawan, Sadong, Belaga, Silantek Formations) (Breitfeld et al., 2017; Galin et al., 2017; Breitfeld and Hall, 2018; Hennig-Breitfeld et al., 2019).

The overlying Kakus Unit is dominated by Lower Cretaceous zircons, with relatively few Precambrian zircons (Fig. 12), indicating a significant change in provenance from the underlying Nyalau Formation. We interpret this to indicate that by the late Early Miocene the dominant source was southern Borneo and input from the west had almost completely ceased. Sediments were most likely derived by uplift and recycling of Rajang Group/Kuching Supergroup sediments from Borneo, which have abundant Lower Cretaceous zircons (Galin et al., 2017; Breitfeld and Hall, 2018). The Kakus Unit also has a very similar detrital zircon age distribution and heavy mineral assemblage to samples from the Balingian and Begrih Formations (Figs. 11 and 14) reported by Hennig-Breitfeld (2019). We therefore interpret the Kakus Unit as an equivalent of the Balingian Formation (Fig. 3), rather than as part of the Nyalau Formation as suggested by Liechti et al. (1960).

The youngest zircons found in the samples range from c. 19 to 31 Ma and are likely to be sourced from Borneo. Zircon U-Pb ages from the Sintang Suite range between c. 18 to 24 Ma (Breitfeld et al., 2019). This phase of magmatism was possibly related to deformation and exhumation of central Borneo reported by Moss et al. (1998), Davies et al. (2014) and Breitfeld et al. (2017) at c. 25 to 30 Ma.

9.3. Implications for drainage system

The early Cenozoic drainage system in Borneo experienced several major changes with river reversals and shifts of dominant source regions. In the early Paleogene, a proto-Sarawak river system carried sediment from East Malaya, Sibumasu and SW Borneo (Fig. 15a), and intermittently from SW Borneo only (Fig. 15b) (Galin et al., 2017; Breitfeld and Hall, 2018), depositing the Kuching Supergroup and its deep marine Rajang Group equivalent. The drainage area of the proto-Sarawak system began to shrink in the late Middle to Late Eocene and was eliminated in the Late Eocene (Hennig-Breitfeld et al., 2019) (Fig. 15c). The Rajang Unconformity at c. 37 Ma marks this major change and in the Sibu and Miri

Zones there was a change from deep/open marine to fluvial-shallow marine deposition (Galin et al., 2017; Hennig-Breitfeld et al. 2019). Sedimentation resumed in the Early Oligocene with the lower Tatau Formation (Rangsi Conglomerate) that formed the lowermost part of the Tatau-Nyalau sedimentary basin that developed on top of the Rajang Group succeeded by thick fluvio-deltaic deposits (Wolfenden, 1960; Hennig-Breitfeld et al., 2019). The Rangsi Conglomerate was derived from very proximal uplifted Rajang Group (Hennig-Breitfeld et al., 2019) (Fig. 15d). A new drainage system established after deposition of the Rangsi Conglomerate that was mainly sourced from East Malaya (including the Bintan Islands and Singapore) and Indochina, indicated by heavy mineral assemblages (Fig. 11) and detrital zircon ages (Fig. 14) different from the older sediments, and carried sediment down the Sunda River (Hennig-Breitfeld et al., 2019), delivered to the upper Tatau, Buan and Nyalau Formations, as well as the open marine Setap Shale Formation with its contemporaneous equivalents (Fig. 16a). The upper Tatau Formation and the Nyalau Formation have heavy mineral assemblages with similar proportions of zircon, TiO_2 polymorphs and tourmaline (Fig. 11), and comparable zircon age populations (Fig. 14). The Crocker Formation of Sabah might represent the slope deposits of that system as they have similar geochronological characteristics (van Hattum et al., 2013, Fig. 14). U-Pb detrital zircon ages from Miocene sediments in the offshore Vietnam Cuu Long and Nam Con Son basins (Hennig et al., 2017b; Hennig and Breitfeld, 2018) are very similar to those of the Nyalau Formation and suggest similar sources. It is also possible that previously deposited sediments in the offshore East Malaya region with an Indochina signature were recycled in the Oligocene into the Nyalau Formation (Fig. 16a).

We suggest that along with the Sunda River another system, the proto-Rajang River, was active in the Oligocene-Early Miocene that flowed from uplifted Borneo, transporting material towards the north and depositing the Merit-Pila Formation in central Borneo (Fig. 16a). In the late Early or Middle Miocene, the proto-Rajang River replaced the Sunda River as the major fluvial system in NW Borneo (Fig. 16b) evident by the diminished Permian-Triassic zircon populations and the increase in Cretaceous Borneo-derived zircons. The similarities of the heavy mineral assemblages (Fig. 11) and detrital zircon ages from the Merit-Pila Formation and the Kakus Unit suggest that they were part of the same or a similar depositional system. A proto-Rajang River delta possibly deposited the Balingian and Begrih Formations and other sediments in the Miri Zone (e.g. Tukau Formation), as well as the Belait Formation on Labuan, that have similar heavy mineral assemblages and zircon age populations (Fig. 14; Nagarajan et al., 2017; Hennig-Breitfeld et al., 2019). This change in provenance also coincides with a change in coastline from a NW-SE to a NE-SW orientation similar to the present-day (Hageman, 1987; Hutchison, 2005; Madon et al., 2013; Hennig-Breitfeld et al., 2019). A possible cause for this reorganisation of the drainage system was the opening of the southwestern end of the South China Sea to cut off the Sunda River system, accompanied by uplift in Borneo which provided material for the growing proto-Rajang River system.

9.4. Correlation with offshore Sarawak and tectonic interpretation

The stratigraphy of offshore Sarawak is generally subdivided into a number of cycles which are the equivalent of the formations identified onshore. There have been a number of publications on the age and boundaries of each cycle but no agreement on the exact age ranges (e.g. Ho, 1978; Hageman et al., 1987; Mat-Zin and Tucker, 1999; Hutchison, 2005; Krebs, 2011; Madon et al., 2013; Lunt and Madon, 2017).

The lowest units are named pre-Cycle I and are referred to as basement (Madon et al., 2013). These are considered to be equivalent to the Rajang Group sediments that underlie the Miri Zone and pre-date the Rajang Unconformity which marks the change from deep marine to inner neritic environments at c. 37 Ma (Hall and Breitfeld, 2017; Hennig-Breitfeld et al., 2019). Cycle I is interpreted to comprise the sediments above this unconformity that range in age from c. 37 to 22.5 Ma (Madon et al., 2013). On land the unconformity is overlain by the fluvio-deltaic Tatau Formation, the shallow marine-dominated Buan Formation and lower part of the tidal-fluvio-deltaic Nyalau Formation (Biban Sandstone Member). The Tatau and the Buan Formations and Biban Sandstone Member broadly correspond to the time range of Cycle I (Early to Late Oligocene), although it should be noted that the onshore stratigraphy is quite heterogeneous and does not correspond to a single sediment package of Cycle I as identified offshore, suggesting there could be deposits above the Rajang Unconformity and below Cycle I.

Cycle II ranges broadly from 22.5 to 18/17.5 Ma (Madon et al., 2013), which corresponds to the upper part of the Nyalau Formation (Upper Nyalau Member) and the boundary between Cycles I and II is interpreted as an unconformity, named the Base Miocene Unconformity (BMU) (Madon et al., 2013). A tectonic event of similar age is the jump of the South China Sea spreading centre towards the south, which occurred at c. 25 Ma (Barckhausen et al., 2014) or 23.6 Ma (Li et al., 2014). On land there is a change from prominent ridges formed by thick sandstone-dominated channels of the Biban Sandstone Member to a more heterolithic-dominated succession of the Upper Nyalau Member. However, no unconformity between the two members of the Nyalau Formation has been identified in this study.

Cycle III ranges from c. 18 to 15 Ma (Madon et al., 2013). Onshore Cycle III equivalents could be the Balingian Formation, possibly the Kakus Unit, the Lower Belait Formation on Labuan, and the lower parts of the post-Nyalau deposits in the northern Miri Zone (e.g. Lambir Formation). The base of these formations on land is the Nyalau Unconformity of c. 17 Ma age (Hennig-Breitfeld et al., 2019). The Nyalau Unconformity has a similar age to the EMU (Early Miocene Unconformity) of offshore Sarawak of Krebs (2011) interpreted by Madon et al. (2013) as c. 19 to 16.5 Ma. This could correlate with the end of spreading in the South China Sea (Li et al., 2014) and be linked to collision in Sabah and uplift of central Borneo, increasing sediment input into the proto-Rajang River system.

Cycle IV ranges from c. 15.5 to 11.5 Ma (Madon et al., 2013), and correlates with the onshore Begrih and Liang Formations (Mukah-Balingian area) in Sarawak and the Middle and Upper Belait Formations on Labuan. Cycle V ranges from c. 11.5 to 5 Ma and consists of marine sands and carbonates (Madon et al., 2013). Equivalents in onshore Sarawak are potentially the Tukau Formation and the Liang Formation (in the Miri area), which might be even younger.

10. Conclusions

The two most important Paleogene to Early Miocene unconformities in onshore Sarawak are the Rajang Unconformity, which marks the end of deep marine deposition at c. 37 Ma, and the Nyalau Unconformity at c. 17 Ma, which is marked by a major switch in sediment provenance.

The Sunda region was drained primarily by the Proto-Sarawak River until c. 37 Ma. After major uplift and deformation of the Rajang Group the Rangsi Conglomerate was deposited. These conglomerates and sandstones are the oldest sediments in the Tatau-Nyalau province and had a local provenance. By c. 30 Ma the Tatau-Nyalau Basin was sourced by the Sunda River system, supplying material from East Malaya/Indochina across the present-day Sunda Shelf, and this river system was active until approximately 17 Ma (Hennig-Breitfeld et al., 2019). A second large river system was active during the 30 to 17 Ma interval, bringing material from south and central Borneo towards the north. This is named here the proto-Rajang River.

At c. 17 Ma there was a major change in the depositional systems in NW Borneo, marked by the Nyalau Unconformity at the top of the Sunda River Delta sediments. The Sunda River supply terminated, probably due to the incision of the Sunda Shelf by the enlarged South China Sea, and sediment was then mainly supplied from Borneo to the prograding proto-Rajang River delta. There was a distinct change in provenance from a predominantly Indochina-Sundaland source for the Nyalau Formation to a predominantly Borneo source for the Kakus Unit. This change was associated with a change in coastline from a NW-SE to a NE-SW orientation similar to the present-day. Sediments of the Mukah-Balingian area (and the Belait Formation on Labuan) are similar to the Kakus Unit and suggest this Borneo source remained dominant until at least the Late Miocene or Pliocene, when the stratigraphic record on land ends.

Acknowledgements

This project was funded by the SE Asia Research Group of Royal Holloway University of London, which is supported by a consortium of oil companies. The Economic Planning Unit of Malaysia and the State

Planning Unit of Malaysia made the fieldwork possible, and the Mineral and Geoscience Department Malaysia, Sarawak assisted in the field and with the logistics. Liew Shan Hian is therefore especially thanked. Richard Mani Banda and Enggong Aji are thanked for their cooperation in conducting the fieldwork. We thank Martin Rittner and Andy Carter (UCL/Birkbeck College) for help and support at the LA-ICP-MS facility and Andy Beard (UCL/Birkbeck College) for help with cathodoluminescence imaging. For their helpful and thorough comments we thank reviewers Clive Burrett and Chris Morley, as well as Khin Zaw for editorial assistance. Carita Augustsson is thanked for helpful comments on an earlier version of this manuscript.

References

Abdelghany, O., 2002. Lower Miocene stratigraphy of the Gebel Shabrawet area, north Eastern desert Egypt. Journal of African Earth Sciences 34, 203-212.

Abdullah, W.H., 2001. A petrographic comparison of oil-generating coals from the tropics and non oil-generating coals from the arctic. Geological Society of Malaysia Annual Geological Conference 2001, 33-38.

Adams, C.G., 1963. The age and foraminiferal fauna of the Bukit Sarang Limestone, Sarawak, Malaysia. Borneo Region, Malaysia Geological Survey Annual Report: 156-162.

Allen, G.P., Chambers, J.L.C., 1998. Sedimentation in the modern and Miocene Mahakam Delta. Indonesian Petroleum Association, 236 pp.

Andersen, T., 2002. Correction of common lead in U–Pb analyses that do not report ^{204}Pb. Chemical Geology 192(1), 59-79.

Asis, J., Jasin, B., 2015. Miocene larger benthic foraminifera from the Kalumpang Formation in Tawau, Sabah. Sains Malaysiana 44, 1397-1405.

Bailey, S.W., Weege, R.J., Cameron, E.N., Spedden, H.R., 1956. The alteration of ilmenite in beach sands. Economic Geology 51(3), 263-279.

Banda, R.M., Honza, E., 1997. Miocene stratigraphy of northwest Borneo Basin. Bulletin of the

Geological Society of Malaysia 40, 1-11.

Banner, F.T., Hodgkinson, R.L., 1991. A revision of the foraminiferal subfamily Heterosteginae. Revista Española de Micropaleontología 23, 101-140.

Barckhausen, U., Engels, M., Franke, D., Ladage, S., Pubellier, M., 2014. Evolution of the South China Sea: revised ages for breakup and seafloor spreading. Marine and Petroleum Geology 58, 599-611.

Benton, M.J., Harper, D.A.T., 1997. Basic Palaeontology. Prentice Hall, Upper Saddle River, N.J., 342 pp.

BouDagher-Fadel, M.K., 2015. Biostratigraphic and geological significance of planktonic foraminifera (Updated 2nd Edition). UCL Press, London, 298 pp.

BouDagher-Fadel, M.K., 2018a. Evolution and geological significance of larger benthic foraminifera. UCL Press, London, 693 pp.

BouDagher-Fadel, M.K., 2018b. Revised diagnostic first and last occurrences of Mesozoic and Cenozoic planktonic foraminifera. UCL Office of the Vice-Provost Research, Professional Papers Series(2), 1-5.

BouDagher-Fadel, M.K., Banner, F.T., 1999. Revision of the stratigraphic significance of the Oligocene-Miocene “Letter-Stages”. Revue de micropaléontologie 42, 93-97.

BouDagher-Fadel, M.K., Lokier, S.W., 2005. Significant Miocene larger foraminifera from south central Java. Revue de Paléobiologie 24, 291-309.

BouDagher-Fadel, M.K., Price, G.D., 2010. Evolution and paleogeographic distribution of the lepidocyclinids. The Journal of Foraminiferal Research 40, 79-108.

BouDagher-Fadel, M.K., Price, G.D., 2013. The phylogenetic and palaeogeographic evolution of the miogypsinid larger benthic foraminifera. Journal of the Geological Society 170, 185-208.

BouDagher-Fadel, M.K., Price, G.D., 2014. The phylogenetic and palaeogeographic evolution of the nummulitoid larger benthic foraminifera. Micropaleontology 483-508.

Breitfeld, H.T., Hall, R., 2018. The eastern Sundaland margin in the latest Cretaceous to Late Eocene:

Sediment provenance and depositional setting of the Kuching and Sibu Zones of Borneo. Gondwana Research 63, 34-64.

Breitfeld, H.T., Hall, R., Galin, T., Forster, M.A., BouDagher-Fadel, M.K., 2017. A Triassic to Cretaceous Sundaland–Pacific subduction margin in West Sarawak, Borneo. Tectonophysics 694, 35-56.

Breitfeld, H.T., Hall, R., Galin, T., BouDagher-Fadel, M.K., 2018. Unravelling the stratigraphy and sedimentation history of the uppermost Cretaceous to Eocene sediments of the Kuching Zone in West Sarawak (Malaysia), Borneo. Journal of Asian Earth Sciences 160, 200-223.

Breitfeld, H.T., Macpherson, C., Hall, R., Thirlwall, M., Ottley, C.J., Hennig-Breitfeld, J., 2019. Adakites without a slab: Remelting of hydrous basalt in the crust and shallow mantle of Borneo to produce the Miocene Sintang and Bau Suite magmatism of West Sarawak. Lithos 344-355, 100-121.

Chaproniere, G.C.H., 1975. Palaeoecology of Oligo-Miocene larger Foraminiferida, Australia. Alcheringa 1, 37-58.

Chaproniere, G.C.H., 1984. The Neogene larger foraminiferal sequence in the Australian and New Zealand regions, and its relevance to the East Indies letter stage classification. Palaeogeography, Palaeoclimatology, Palaeoecology 46, 25-35.

Cohen, K.M., Finney, S.C., Gibbard, P.L. and Fan, J.-X., 2013 (updated 2017). The ICS International Chronostratigraphic Chart. Episode 36, 199-204.

Dalrymple, R.W., Choi, K., 2007. Morphologic and facies trends through the fluvial–marine transition in tide-dominated depositional systems: a schematic framework for environmental and sequence-stratigraphic interpretation. Earth-Science Reviews 81(3), 135-174.

Dashtgard, S.E., 2011. Linking invertebrate burrow distributions (neoichnology) to physicochemical stresses on a sandy tidal flat: implications for the rock record. Sedimentology 58(6), 1303-1325.

Davies, L., Hall, R., Armstrong, R., 2014. Cretaceous crust in SW Borneo: petrological, geochemical and geochronological constraints from the Schwaner Mountains, Proceedings Indonesian Petroleum Association, 38th Annual Convention and Exhibition, IPA14-G-025.

De Boer, N.P., Milroy, W.V., 1952. Geology of the Balingian-Bintulu-Rajang Area. Sarawak Oilfields Limited.

Dickinson, W.R., Beard, L.S., Brakenridge, G.R., Erjavec, J.L., Ferguson, R.C., Inman, K.F., Knepp, R.A., Lindberg, F.A. , Ryberg, P.T., 1983. Provenance of North American Phanerozoic sandstones in relation to tectonic setting. Geological Society of America Bulletin 94(2), 222-235.

Dill, H.G., 2001. The geology of aluminium phosphates and sulphates of the alunite group minerals: a review. Earth-Science Reviews 53(1), 35-93.

Dill, H.G., Melcher, F., Füßl, M., Weber, B., 2007. The origin of rutile-ilmenite aggregates ("nigrine") in alluvial-fluvial placers of the Hagendorf pegmatite province, NE Bavaria, Germany. Mineralogy and Petrology 89(3), 133-158.

Doutch, H.F., 1992. Aspects of the structural histories of the Tertiary sedimentary basins of East, Central and West Kalimantan and their margins. BMR Journal of Australian Geology and Geophysics 13, 237-250.

Drooger, C.W., 1993. Radial Foraminifera; morphometrics and evolution,del 41, Verhandelingen der Koninklijke Akademie van Wetenschappen. Afdeeling Natuurkunde. Erste Reeks, Amsterdam, 241 pp.

Eames, F.E., Banner, F.T., Blow, W.H., Clarke, W.J., 1962. Fundamentals of Mid-Tertiary Stratigraphical Correlation, Cambridge University Press, Cambridge 163 pp.

Feldman, H., Demko, T., 2015. Recognition and prediction of petroleum reservoirs in the fluvial/tidal transition. In: P.J. Ashworth, J.L. Best and D.R. Parsons (Editors), Fluvial-Tidal Sedimentology. Developments in Sedimentology 68. Elsevier, pp. 483-528.

Ferrandini, M., BouDagher-Fadel, M.K., Ferrandini, J., Oudet, J., Andre, J.-P., 2010. New observations about the Miogypsinidae of the Early and Middle Miocene of Provence and Corsica (France) and northern Sardinia (Italy). Annales de Paleontologie 96, 67-94.

Fyhn, M.B.W., Green, P.F., Bergman, S.C., Van Itterbeeck, J., Tri, T.V., Dien, P.T., Abatzis, I., Thomsen, T.B., Chea, S., Pedersen, S.A.S., 2016. Cenozoic deformation and exhumation of the Kampot Fold Belt and implications for south Indochina tectonics. Journal of Geophysical Research: Solid Earth 121, 5278-5307.

Galin, T., Breitfeld, H.T., Hall, R., Sevastjanova, I., 2017. Provenance of the Cretaceous–Eocene Rajang Group submarine fan, Sarawak, Malaysia from light and heavy mineral assemblages and U-Pb zircon geochronology. Gondwana Research 51, 209-233.

Gradstein, F.M., Ogg, J.G., Schmitz, M., Ogg, G., 2012. The Geologic Time Scale 2012. Elsevier, 1144 pp.

Griffin, W.L., W.L., Powell, W.J., Pearson, N.J., O'Reilly, S.Y., 2008. GLITTER: data reduction software for laser ablation ICP-MS. In: P.J. Sylvester (Editor), Laser Ablation ICP-MS in the Earth Sciences: Current practices and outstanding issues. Short Course Series Mineralogical Association of Canada, pp. 308-311.

Hageman, H., 1987. Paleobathymetrical changes in NW Sarawak during Oligocene to Pliocene. Geol. Soc. Malaysia, Bulletin 21, 91-102.

Hageman, H., Lesslar, P., Fon, W.C., 1987. Revised biostratigraphy of Oligocene to Recent deposits of Sarawak and Sabah (unpublished report). Sarawak Shell Berhad.

Haile, N.S., 1962. The geology and mineral resources of Suai-Baram area, North Sarawak. Geological Survey Department British Territories in Borneo, Memoir 13, 176 pp.

Haile, N.S., 1974. Borneo. In: A.M. Spencer (Editor), Mesozoic-Cenozoic Orogenic Belts. Geological Society of London Special Publication, pp. 333-347.

Hall, R., Breitfeld, H.T., 2017. Nature and demise of the Proto-South China Sea. Geological Society of Malaysia, Bulletin 63, 61-76.

Hassan, M.H.A., Johnson, H.D., Allison, P.A., Abdullah, W.H., 2013. Sedimentology and stratigraphic development of the upper Nyalau Formation (Early Miocene), Sarawak, Malaysia: a mixed wave-and tide-influenced coastal system. Journal of Asian Earth Sciences 76, 301-311.

Heng, Y.E., 1992. Geological Map of Sarawak, 1:500,000. Geological Survey of Malaysia.

Hennig, J,. Breitfeld, H.T., 2018. Sources of Cenozoic Sediments around the Southern South China Sea, Proceedings of the 2018 South East Asia Petroleum Exploration Society (SEAPEX). Asia-Pacific E&P Conference, London, pp. 17. (Abstract & poster).

Hennig, J., Breitfeld, H.T., Hall, R., Nugraha, A.M.S., 2017a. The Mesozoic tectono-magmatic evolution at the Paleo-Pacific subduction zone in West Borneo. Gondwana Research 48, 292-310.

Hennig, J., Breitfeld, H.T., Gough, A., Hall, R., Long, T.V., Kim, V.M., Quang, S.D., 2017b. SE Vietnam U-Pb zircon ages and provenance: Correlating the Da Lat Zone on land with the Cuu Long Basin offshore, AGU Fall Meeting 2017, New Orleans, USA. (Abstract & poster).

Hennig, J., Breitfeld, H.T., Gough, A., Hall, R., Long, T.V., Kim, V.M., Quang, S.D, 2018. U-Pb zircon ages and provenance of upper Cenozoic sediments from the Da Lat Zone, SE Vietnam: implications for an intra-Miocene unconformity and paleo-drainage of the proto-Mekong River. Journal of Sedimentary Research 88(4), 495-515.

Hennig-Breitfeld, J., Breitfeld, H.T., Hall, R., BouDagher-Fadel, M., Thirlwall, M., 2019. A new upper Paleogene to Neogene stratigraphy for Sarawak and Labuan in northwestern Borneo: Paleogeography of the eastern Sundaland margin. Earth-Science Reviews 190, 1-32.

Hennig-Breitfeld, J., Breitfeld, H.T., Hall, R., BouDagher-Fadel, M., in press. Reply to Discussion: Hennig-Breitfeld, J., H.T. Breitfeld, R. Hall, M. BouDagher-Fadel, and M. Thirlwall. 2019. A new upper Paleogene to Neogene stratigraphy for Sarawak and Labuan in northwestern Borneo: Paleogeography of the eastern Sundaland margin. Earth-Science Reviews 190, 1–32. Earth-Science Reviews 103066.

Ho, K.F., 1978. Stratigraphic framework for oil exploration in Sarawak. Geol. Soc. Malaysia, Bull. 10, 1-13.

Hutchison, C.S., 2005. Geology of North-West Borneo. Sarawak, Brunei and Sabah. Elsevier, Amsterdam, Netherlands, 421 pp.

Isnaniawardhani, V., 2018. Larger foraminifera catalog on member of calcarenite Pamutuan Formation. (Katalog Foraminifera Besar pada Anggota Kalkarenit Formasi Pamutuan), Unpad Press, Bandung, 117 pp.

Jordi, H.A., Bowen, J.M., 1956. Geological Reconnaissance of the Rajang Area; with Appendix: Palaeontology of the Rajang Area by J.V. John, GR690 (unpublished report).

Kessler, F.L. and Jong, J., 2015. Tertiary uplift and the Miocene evolution of the NW Borneo shelf margin. Berita Sedimentologi 33, 21-46.

Kho, C.H., 1968. Bintulu Area, Central Sarawak, East Malaysia: Explanation of sheet 3/113/13, Report 5. Geological Survey, Borneo Region, Malaysia.

Kirk, H.J.C., 1957. The geology and mineral resources of the upper Rajang and adjacent areas. British Territories Borneo Region Geological Survey, Memoir 8, 181pp.

Konzalová, M., 2005. Micropalaeontologický výzkum Merit – Pila, Sarawak. MSci thesis, Institute of Geology of the Czech Academy of Sciences, Praha.

Krebs, W.N., 2011. Upper Tertiary chronosequence stratigraphy of offshore Sabah and Sarawak, NW Borneo, Malaysia: A unified scheme based on graphic correlation. Bull. Geol. Soc. Malaysia 57, 39-46.

Labourdette, R., Jones, R.R., 2007. Characterization of fluvial architectural elements using a three-dimensional outcrop data set: Escanilla braided system, South-Central Pyrenees, Spain. Geosphere 3(6), 422-434.

Lee, C.P., Leman, M.S., Nasib, B.M., Karim, R., 2004. Stratigraphic lexicon of Malaysia. Geological Society of Malaysia, 162 pp.

Li, C.F., Xu, X., Lin, J., Sun, Z., Zhu, J., Yao, Y., Zhao, X., Liu, Q., Kulhanek, D.K. , Wang, J., 2014. Ages and magnetic structures of the South China Sea constrained by deep tow magnetic surveys and IODP Expedition 349. Geochemistry, Geophysics, Geosystems 15(12), 4958-4983.

Liaw, K.K., 1987. Evaluation of the coal resources of the Merit Block, Merit Pila Coal Field, Sarawak. Economic Geology Bulletin, 3. Ministry of Primary Industries, Malaysia, Kuala Lumpur, Malaysia, 131 pp.

Liechti, P., Roe, F.W., Haile, N.S., 1960. The Geology of Sarawak, Brunei and the western part of North Borneo. British Territories of Borneo, Geological Survey Department, Bulletin (Two volumes) 3, 360pp.

Lunt, P., Madon, M., 2017. A review of the Sarawak Cycles: History and modern application. Bulletin of the Geological Society of Malaysia 63, 77-101.

Madon, M., Kim, C.L., Wong, R., 2013. The structure and stratigraphy of deepwater Sarawak, Malaysia: implications for tectonic evolution. Journal of Asian Earth Sciences, 76: 312-333.

Mange, M.A. and Maurer, H.F.W., 1992. Heavy minerals in colour. Chapman & Hall, London, 147 pp.

Mange, M.A., Wright, D.T. (Editors), 2007. Heavy minerals in use. Developments in Sedimentology, 58. Elsevier, Amsterdam, 1283 pp.

Martin, C.A.L., Turner, B.R., 1998. Origins of massive-type sandstones in braided river systems. Earth-Science Reviews 44(1), 15-38.

Mat-Zin, I.C., Tucker, M.E., 1999. An alternative stratigraphic scheme for the Sarawak Basin. Journal of Asian Earth Sciences 17, 215-232.

McCabe, P.J., 1987. Facies studies of coal and coal-bearing strata. Geological Society, London, Special Publications 32(1), 51-66.

McGilvery, T.A., Cook, D.L., 2003. The influence of local gradients on accommodation space and linked depositional elements across a stepped slope profile, offshore Brunei. In: H.H. Roberts, N.C. Rosen, R.H. Fillon and J.B. Anderson (Editors), Shelf margin deltas and linked down slope petroleum systems: Global significance and future exploration potential. Gulf Coast Section SEPM, pp. 387-419.

Meiburg, E., Kneller, B., 2010. Turbidity currents and their deposits. Annual Review of Fluid Mechanics 42, 135-156.

Miall, A.D., 1985. Architectural-element analysis: A new method of facies analysis applied to fluvial deposits. Earth Science Reviews 22, 261-308.

Mihaljević, M., Renema, W., Welsh, K., Pandolfi, J.M., 2014. Eocene–Miocene shallow-water carbonate platforms and increased habitat diversity in Sarawak, Malaysia. PALAIOS 29(7), 378-391.

Morton, A.C., Hallsworth, C.R., 1994. Identifying provenance-specific features of detrital heavy mineral assemblages in sandstones. Sedimentary Geology 90, 241-256.

Moss, S.J., Carter, A., Baker, S., Hurford, A.J., 1998. A Late Oligocene tectono-volcanic event in East Kalimantan and the implications for tectonics and sedimentation in Borneo. Journal of the Geological Society 155, 177-192.

Mücke, A., Chaudhuri, J.N.B., 1991. The continuous alteration of ilmenite through pseudorutile to leucoxene. Ore geology reviews 6(1), 25-44.

Nagarajan, R., Roy, P.D., Kessler, F.L., Jong, J., Dayong, V., Jonathan, M.P., 2017. An integrated study of geochemistry and mineralogy of the Upper Tukau Formation, Borneo Island (East Malaysia): Sediment provenance, depositional setting and tectonic implications. Journal of Asian Earth Sciences 143, 77-94.

Nemchin, A.A., Cawood, P.A., 2005. Discordance of the U–Pb system in detrital zircons: implication for provenance studies of sedimentary rocks. Sedimentary Geology 182(1-4), 143-162.

Nguyen, H.H., Carter, A., Van Hoang, L., Vu, S.T., 2018. Provenance, routing and weathering history of heavy minerals from coastal placer deposits of southern Vietnam. Sedimentary Geology 373, 228-238.

Nguyen, T.T.B., Satir, M., Siebel, W., Chen, F., 2004. Granitoids in the Dalat zone, southern Vietnam: age constraints on magmatism and regional geological implications. International Journal of Earth Sciences 93(3), 329-340.

Nugraheni, R.D., Chow, W.S., Rahman, A.H.A., Nazor, S.N.M., Abdullah, M.F., 2014. Tertiary coal-bearing heterolithic packages as low permeability reservoir rocks in the Balingian Sub-basin, Sarawak, Malaysia. Bull. Geol. Soc. Malaysia 60, 85-93.

Osvald, P., Sýkorová, I., 2006. Merit Pila coal basin, Malaysia - geology and coal petrology, International Symposium on Lower Rank Coal, Bandung: Ministry of Energy and Mineral Resources, pp. 16-17. (Abstract).

Özcan, E., Less, G.r., 2009. First record of the co-occurrence of western Tethyan and Indo-Pacific larger foraminifera in the Burdigalian of the Mediterranean province. The Journal of Foraminiferal Research 39, 23-39.

Pearce, N.J.G., Perkins, W.T., Westgate, J.A., Gorton, M.P., Jackson, S.E., Neal, C.R. , Chenery, S.P., 1997. A Compilation of New and Published Major and Trace Element Data for NIST SRM 610 and NIST SRM 612 Glass Reference Materials. Geostandards Newsletter 21(1), 115-144.

Quijada, I.E., Suarez-Gonzalez, P., Benito, M.I., Mas, R., 2016. Tidal versus continental sandy-muddy flat deposits: evidence from the Oncala Group (Early Cretaceous, N Spain), Contributions to modern and ancient tidal sedimentology: proceedings of the Tidalites 2012 conference. John Wiley & Sons, pp. 133-159.

Raju, D.S.N., 1974. Study of Indian Miogypsinidae. Utrecht Micropaleontological Bulletins 9, 148 pp.

Renema, W., 2007. Fauna Development of Larger Benthic Foraminifera in the Cenozoic of Southeast Asia. In W. Renema (ed.), Biogeography, Time and Place: Distributions, Barriers and Islands. Topics in Geobiology 29, Springer, 179-215.

Roohi, G., 1998. Biostratigraphy and Paleoecology of the Subis Limestone,(Early Miocene) Sarawak, East Malaysia and Correlation with the Neogene of the Indus Basin, Pakistan. Pakistan Journal of Hydrocarbon Research 10, 81-104.

Roozbahani, P., Alp, G., 2011. Lithostratigraphy and biostratigraphy of Oligocene Miocene deposits (Asmari Formation) in South-West Iran (Zagros Basin, northern Khorramabad). Geo Alp 8, 46-55.

Sandal, S.T., 1996. The geology and hydrocarbon resources of Negara Brunei Darussalam. Syabas, Bandar Seri Begawan, Brunei Darussalam, 243 pp.

Searle, M.P., Whitehouse, M.J., Robb, L.J., Ghani, A.A., Hutchison, C.S., Sone, M., Ng, S.W., Roselee, M.H., Chung, S.-L., Oliver, G.J.H., 2012. Tectonic evolution of the Sibumasu-Indochina terrane collision zone in Thailand and Malaysia: constraints from new U-Pb zircon chronology of SE Asian tin granitoids. Journal of the Geological Society 169(4), 489-500.

Sevastjanova, I., Clements, B., Hall, R., Belousova, E.A., Griffin, W.L., Pearson, N., 2011. Granitic magmatism, basement ages, and provenance indicators in the Malay Peninsula: Insights from detrital zircon U-Pb and Hf-isotope data. Gondwana Research 19(4), 1024-1039.

Sevastjanova, I., Hall, R., Alderton, D., 2012. A detrital heavy mineral viewpoint on sediment provenance and tropical weathering in SE Asia. Sedimentary Geology 280, 179-194.

Shellnutt, J.G., Lan, C.-Y., Van Long, T., Usuki, T., Yang, H.-J., Mertzman, S.A., Iizuka, Y., Chung, S.-L., Wang, K.-L. , Hsu, W.-Y., 2013. Formation of Cretaceous Cordilleran and post-orogenic granites and their microgranular enclaves from the Dalat zone, southern Vietnam: Tectonic implications for the evolution of Southeast Asia. Lithos 182, 229-241.

Simmons, M.D., Bidgood, M.D., Brenac, P., Crevello, P.D., Lambiase, J.J. , Morley, C.K., 1999. Microfossil assemblages as proxies for precise palaeoenvironmental determination—an example from Miocene sediments of northwest Borneo. Geological Society, London, Special Publications 152(1), 219-241.

Sircombe, K.N., 2004. AgeDisplay: an EXCEL workbook to evaluate and display univariate geochronological data using binned frequency histograms and probability density distributions. Computers & Geosciences 30(1), 21-31.

Sláma, J., Košler, J., Condon, D.J., Crowley, J.L., Gerdes, A., Hanchar, J.M., Horstwood, M.S.A., Morris, G.A., Nasdala, L., Norberg, N., Schaltegger, U., Schoene, B., Tubrett, M.N. , Whitehouse, M.J., 2008. Plešovice zircon — A new natural reference material for U–Pb and Hf isotopic microanalysis. Chemical Geology 249(1–2), 1-35.

Suttner, L.J., Basu, A. Mack, G.H., 1981. Climate and the origin of quartz arenites. Journal of Sedimentary Research 51(4), 1235-1246.

Tan Sin Hok, 1932. On the genus Cycloclypeus, Pt.1, and an appendix on the heterostegines of Tjimanggoe, S. Bantam, Java. Wetenschappelijke Mededeelingen van de Dienst van de

Mijnbouw in Nederlandsch-Oost-Indië, 19, 194 pp.

Vakarelov, B.K., Ainsworth, R.B. MacEachern, J.A., 2012. Recognition of wave-dominated, tide-influenced shoreline systems in the rock record: Variations from a microtidal shoreline model. Sedimentary Geology 279, 23-41.

van Hattum, M.W.A., Hall, R., Pickard, A.L., Nichols, G.J., 2013. Provenance and geochronology of Cenozoic sandstones of northern Borneo. Journal of Asian Earth Sciences 76(0), 266-282.

Williams, P.R., Johnston, C.R, Almond, R.A., Simamora, W.H., 1988. Late Cretaceous to Early Tertiary structural elements of West Kalimantan. Tectonophysics 148(3/4), 279-298.

Wolfenden, E.B., 1960. The geology and mineral resources of the lower Rajang Valley and adjoining areas, Sarawak. British Territories Borneo Region Geological Survey Department, Memoir 11, 167pp.

Figure captions

Fig. 1: Tectonic provinces of western Borneo (modified after Haile, 1974; Hennig et al., 2017a; Breitfeld and Hall, 2018). The red box shows the research area in the Miri Zone.

Fig. 2: Geological map of the research area in the southern Miri Zone (modified from Liechti et al., 1960; Heng, 1992; Hennig-Breitfeld et al., 2019) with sample locations. F = Fault.

Fig. 3: Stratigraphy of the Miri Zone (modified from Liechti et al., 1960; Hutchison, 2005; Hall and Breitfeld, 2017; Hennig-Breitfeld et al., 2019, in press) and correlation to the offshore cycles (based on Madon et al., 2013). Samples with their approximate relative stratigraphic position: 1 – TB52, 2 – TB51, 3 – Ny-03, 4 – Ny-07, 5 – Ny04-06, 6 – TB50, 7 – Ny-01, 8 – TB244, 9 – TB243, 10 – Sub-01, 11 – Set-01 (all this study); 12 – TB200a (from Hennig-Breitfeld et al., 2019). Sarawak Cycles after Madon et al. (2013) and Far East Letter Stages and Planktonic zones after BouDagher-Fadel (2015, 2018). Cgl. = conglomerate, Lmst = limestone, TCU = Top Crocker unconformity, U = unconformity, Liang-M =

Liang Formation in Mukah province (the Liang Formation near Miri and in Brunei is a significantly younger different formation).

Fig. 4: Field photographs of the Biban Sandstone Member (a and b) and Upper Nyalau Member (c to g). a) Sandstone channels cut into heterolithic beds. b) Heterolithic bed with ripple to flaser bedding dissected by medium grained sandstone. Several up to 10 cm long inclined sand-filled tubes indicate *Skolithos*. c) Massive sandstone beds with some horizontal lamination at the base overlain by rippled sandstone and heterolithic bed at the top. d) Mudstone/shale with intercalations of calcareous layers, and thin layers of clastic material. e) Cross-bedded sandstone bed on top of rippled sandstone-mudstone alternations. f) *Cruziana* on the bedding plane. g) Fossiliferous calcareous hard-ground that contained benthic foraminifera and coralline algae fragments (inset).

Fig. 5: Field photographs of the Kakus Unit. a) Shallow inclined alternations of sandstone, siltstone, mudstone and heterolithic beds, overlain by thick carbonaceous mudstone. b) Horizontal laminated alternations of sandstone, siltstone, mudstone and heterolithic beds. The dark colour is due to weathering of carbonaceous mud layers and thin coal seams. c) Asymmetrical and symmetrical rippled sandstone with crudely developed low-angle cross-beds and truncation of sedimentary structures. Colour results from iron oxide Liesegang rings. d) Rippled sandstone with restricted bioturbation and crudely developed planar cross-bedding in the middle of the photograph. e) Moderately bioturbated heterolithic beds with *Skolithos* and *Ophiomorpha*. A single c. 10 cm large *Skolithos* burrow filled with sand is in the upper left side of the image.

Fig. 6: Field photographs of the Merit-Pila Formation. a) Horizontal laminated and rippled sandstone intercalated with well-sorted conglomerates that are typically for the lower part of the formation. b) Massive sandstone bed forms a lateral migrating channel complex of a braided river. c) Well-sorted conglomerate composed predominantly of dark-coloured indurated sandstone clasts derived from the Belaga Formation and some quartz and chert clasts. d) Poorly sorted polymict conglomerate composed of quartz, mudstone, chert and sandstone clasts, cutting erosively into a sandstone bed. e)

Trough cross-bedded sandstone with intercalations of horizontal and inclined conglomerate beds that indicate channels. Newly developed cross-beds truncated over older structures. The package is overlain by a massive c. 20 cm thick polymict conglomerate bed. f) Bedforms in fine-grained sandstone include horizontal lamination, planar cross-bedding and climbing ripples. Tops of crests are formed of carbonaceous mud. g) Discontinuous coal seams and coal fragments in horizontal laminated sandstone. j) Fine-grained grey siltstone grades into c. 1.5 m thick weathered mudstone, overlain sharply by medium-grained sandstone channel. Vegetation covers further sharp alternations of thick mudstone with sandstone beds.

Fig. 7: Field photographs of the Setap Shale Formation and its time equivalents in the northern Miri Zone. a) Shallow inclined mudstone-shale-siltstone alternations of the Setap Shale Formation. b) Large outcrop of fine grained mudstone/shale which contains thin (cm-size) layers of calcareous hard grounds (Setap Shale Formation). c) Subis Limestone cliff at a quarry side at the southeast side of Gunung Subis. d) Stacked small siltstone-sandstone channels (c. 10-30 cm) and siltstone beds in shale-siltstone alternations (Sibuti Formation). e) Contact between the Setap Shale Formation and the overlying Sibuti Formation. The layers are sub-vertical.

Fig. 8: a) *Lepidocyclina stillafera* Scheffen, Ny-04 (Upper Nyalau Member). b) *Austrotrillina asmariensis* Adams, Ny-06a (Upper Nyalau Member). c) *L. (Nephrolepidina) sumatrensis* Brady, Ny-06b (Upper Nyalau Member). d) *Spiroclypeus tidoenganensis* van der Vlerk, Ny-06b (Upper Nyalau Member). e) *Miogypsinodella primitiva* BouDagher-Fadel and Lord, Sub-01a (Subis Limestone). f) *Amphisorus martini* Verbeek, Sub-01a (Subis Limestone). g) *Catapsydrax dissimilis* (Cushman and Bermudez), Set-01a (Setap Shale Formation). h) *Paragloborotalia continuosa (*Blow), Set-01a (Setap Shale Formation). i) *Globigerinoides quadrilobatus* (d'Orbigny), Set-01b (Setap Shale Formation). Scale bars: Figs. a-f = 1 mm; Figs g-i = 0.5 mm.

Fig. 9: a) Sample Ny-06a thin section photomicrograph of (1) *Lepidocyclina* (*Nephrolepidina*) *sumatrensis* Brady, (2) *Miogypsina tani* Drooger, (3) *Miogypsinoides bantamensis* Tan Sin hok. b)

Sample Ny-06b thin section photomicrograph of (1) *Miogypsina kotoi* Hanzawa, (2) *Lepidocyclina* (*Nephrolepidina*) sumatrensis Brady. c) *Miogypsina intermedia* Drooger, sample Sub-01a. Scale bars = 1 mm.

Fig. 10: Light mineral ternary diagrams, showing the composition (after Pettijohn et al., 1987) and the provenance (after Dickinson et al., 1983) of the analysed samples. The Biban Sandstone Member and the Upper Nyalau Member are classed mainly as lithic arenites. Kakus Unit and Merit-Pila Formation samples are classed as sublitharenites. All samples have a recycled orogenic character in the QFL diagram, and plot between mixed, quartzose recycled and transitional recycled fields in the QmFLt diagram.

Fig. 11: Comparison of heavy mineral assemblages of the Tatau-Nyalau Basin with the contemporaneous proto-Rajang samples and the younger Mukah-Balingian sequence. Data for TB54, TA-04, TB200a and TB201 are from Hennig-Breitfeld et al. (2019).

Fig. 12: Age histograms and probability density for detrital zircons of the Nyalau Formation. Biban Sandstone Member and Upper Nyalau Member samples show a dominant Triassic detrital zircon peak, accompanied by Cretaceous and Precambrian (~ 1.8 Ga) peaks. The Kakus Unit sample is dominated by Cretaceous zircons. The left panel displays ages from 0 to 500 Ma and the right from 500 to 4000 Ma. The bin width is 10 Ma for the left panel and 50 Ma for the right.

Fig. 13: Age histograms and probability density for detrital zircons of the Merit-Pila Formation, showing wide Cretaceous, Permian-Triassic, Ordovician-Silurian and Precambrian (~ 0.8-1 Ga, ~ 1.8 Ga, ~ 2.5 Ga) peaks.

Fig. 14: Comparison of age histograms and probability density for the upper Tatau (*Hennig-Breitfeld et al., 2019), Nyalau (Biban Sandstone and Upper Nyalau Members) and Kakus Unit (all this study), Crocker Formation (**van Hattum et al., 2013), coarse-grained samples of the Balingian, Begrih and Lower Belait Formations, and all Mukah-Balingian and Belait samples (*Hennig-Breitfeld et al., 2019). Similarities of detrital zircon ages between the upper Tatau Formation, Biban Sandstone Member and

Upper Nyalau Member, and the Crocker Formation suggest these are part of the same drainage system (Sunda River). Shift of provenance towards a Borneo source in the Kakus Unit and Mukah-Balingian successions and the Belait Formation on Labuan expressed by the dominant Cretaceous age peak. Kakus Unit and coarse samples from the Mukah-Balingian area and from Belait Formation are indistinguishable.

Fig. 15: Paleogeography maps of the NW Borneo/eastern Sundaland drainage system in the a) Paleocene showing the proto-Sarawak River draining East Malaya, Sibumasu, West Borneo and SW Borneo, b) Late Paleocene to Middle Eocene showing the proto-Sarawak River draining only West and SW Borneo, c) Middle to Late Eocene showing the shrinking proto-Sarawak River in its last stages after its capture are included East Malaya, Sibumasu, West Borneo and SW Borneo, and d) Early Oligocene showing the deposition of the lower Tatau (Rangsi Conglomerate) (modified from Breitfeld and Hall, 2018 and after Hennig-Breitfeld et al., 2019). Abbreviations: S – Schwaner Mountains; W – West Borneo; K – Karimunjawa Arch; P – Penian High; R. – River.

Fig. 16: Paleogeography maps and environment block diagrams of the Sunda River and proto-Rajang River in the a) Oligocene to Early Miocene (c. 30 to 17 Ma) with e.g. the Merit-Pila, Setap and Nyalau Formations, and b) in the late Early Miocene to Late Miocene (c. 17 to 10 Ma) with e.g. the Kakus Unit, Belait, Balingian and Lambir Formations. Abbreviations: S – Schwaner Mountains; W – West Borneo; B – Barito; R. – River; SCS – South China Sea; PSCS – Proto-South China Sea. Paleogeography maps based on Hennig-Breitfeld et al. (2019).

Table captions

Tab. 1: Biostratigraphy results from the Nyalau Formation, Subis Limestone (Tangap Formation) and Setap Shale Formation. Age based on the Planktonic Zonation scheme relative to the biostratigraphical time scale (as defined by Gradstein et al., 2012), and correlation to the Shallow benthic zones and the Far East 'letter stages' after BouDagher-Fadel (2018a), and BouDagher-Fadel (2015) and BouDagher-Fadel et al. (2018b).

Tab. 2: Light mineral modes for the Nyalau Formation, Kakus Unit and Merit-Pila Formation. (Qm = monocrystalline non-undulatory quartz, Qmu = monocrystalline undulatory quartz, Qv = volcanic quartz, Qp = polycrystalline quartz, Ch = chert, Fp = plagioclase, Fk = K-feldspar, Lm = metamorphic lithic fragments, Ls = sedimentary lithic fragments, Lv = volcanic lithic fragments, H = heavy minerals, Mt = matrix, Lithics (L) = Lm+Ls+Lv, Total lithic fragments (Lt) = Lm+Ls+Lv+Qp+Ch, Total Qm = Qm+Qmu+Qv, Total Q = Qm+Qmu+Qv+Ch).

Tab. 3: Heavy mineral counts and ratios of the Nyalau Formation, Kakus Unit and Merit-Pila Formation. (ZTR = zircon – tourmaline - rutile index, RZi = TiO_2-polymorphs - zircon index, ZTi = zircon - tourmaline index).

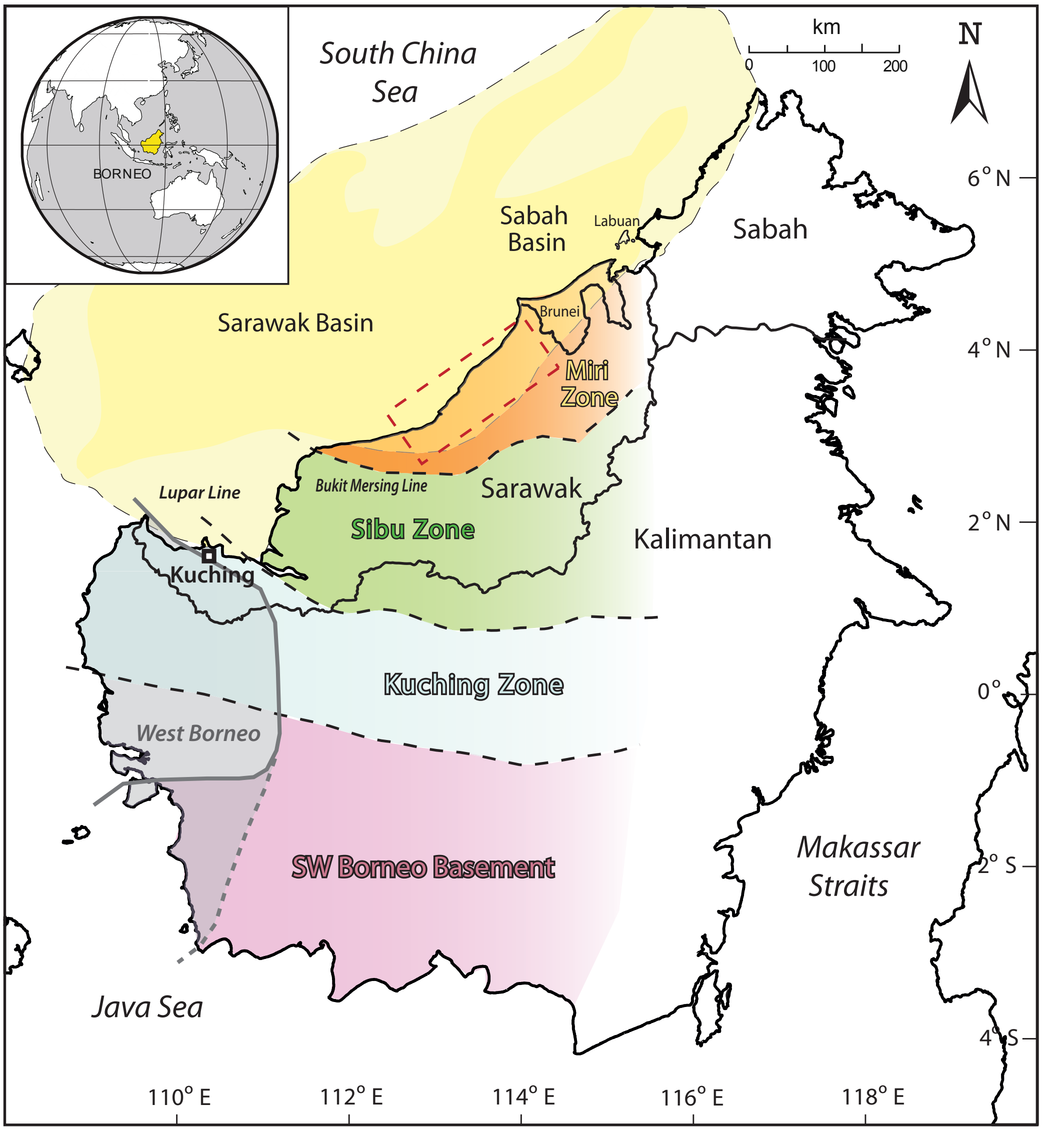
South China
Sea
km
0
100
200
N
BORNEO
6° N
4° N
2° N
0°
2° S
4° S
Sabah
Basin
Labuan
Sabah
Sarawak Basin
Brunei
Miri
Zone
Lupar Line
Bukit Mersing Line
Sarawak
Sibu Zone
Kalimantan
Kuching
Kuching Zone
West Borneo
SW Borneo Basement
Makassar
Straits
Java Sea
110° E
112° E
114° E
116° E
118° E

Fig. 1

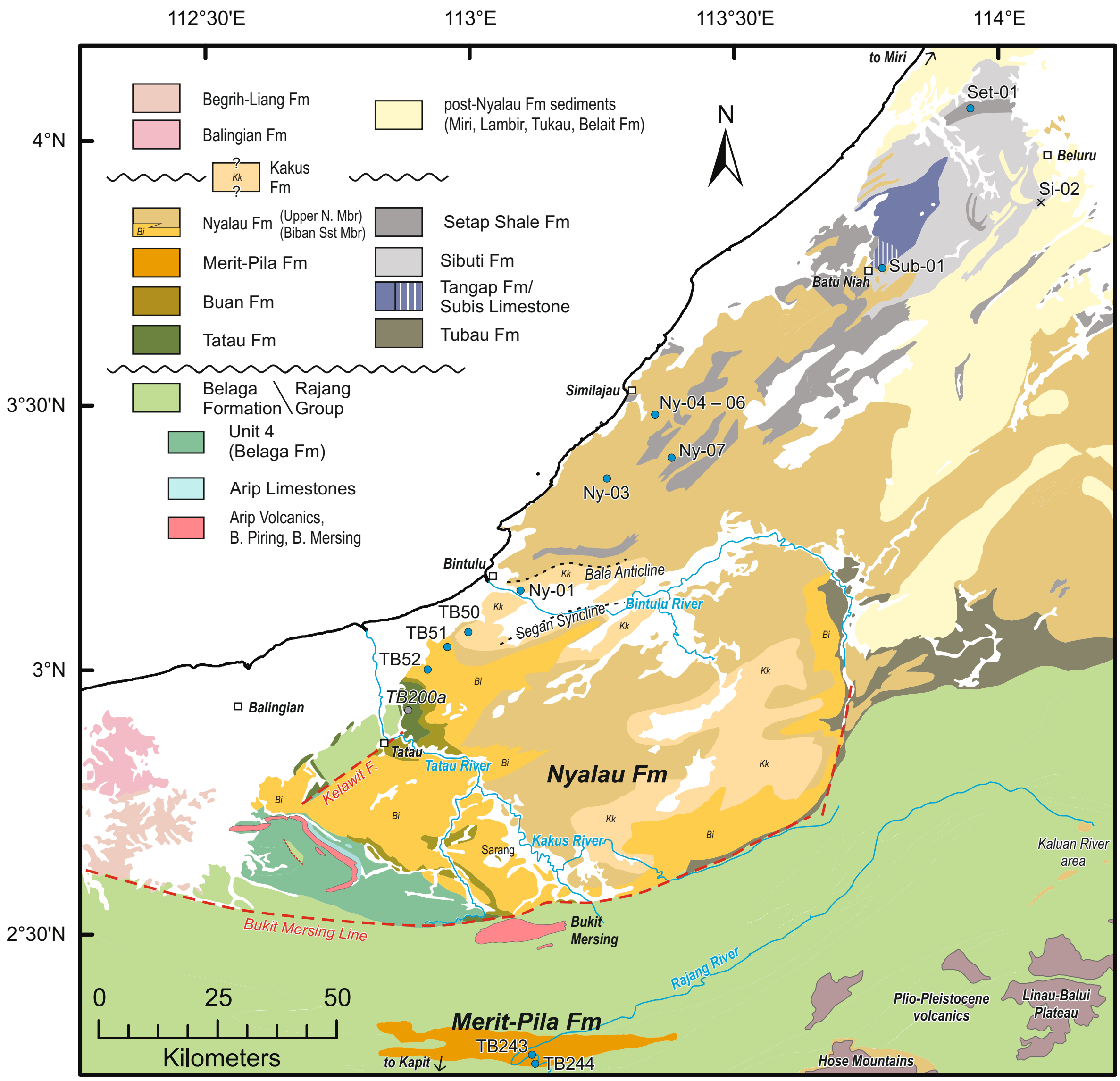

112°30'E
113°E
113°30'E
114°E
4°N
3°30'N
3°N
2°30'N
Begrih-Liang Fm
Balingian Fm
Kakus Fm
Nyalau Fm (Upper N. Mbr) (Biban Sst Mbr)
Merit-Pila Fm
Buan Fm
Tatau Fm
post-Nyalau Fm sediments (Miri, Lambir, Tukau, Belait Fm)
Setap Shale Fm
Sibuti Fm
Tangap Fm/ Subis Limestone
Tubau Fm
Belaga Formation
Rajang Group
Unit 4 (Belaga Fm)
Arip Limestones
Arip Volcanics, B. Piring, B. Mersing
N
to Miri
Set-01
Beluru
Si-02
Sub-01
Batu Niah
Similajau
Ny-04 – 06
Ny-07
Ny-03
Bintulu
Ny-01
Bala Anticline
Segan Syncline
Bintulu River
TB50
TB51
TB52
TB200a
Balingian
Tatau
Tatau River
Kelawit F.
Nyalau Fm
Kakus River
Sarang
Bukit Mersing
Bukit Mersing Line
Kaluan River area
Rajang River
Plio-Pleistocene volcanics
Linau-Balui Plateau
Hose Mountains
Merit-Pila Fm
TB243
TB244
to Kapit
0
25
50
Kilometers

Fig. 2

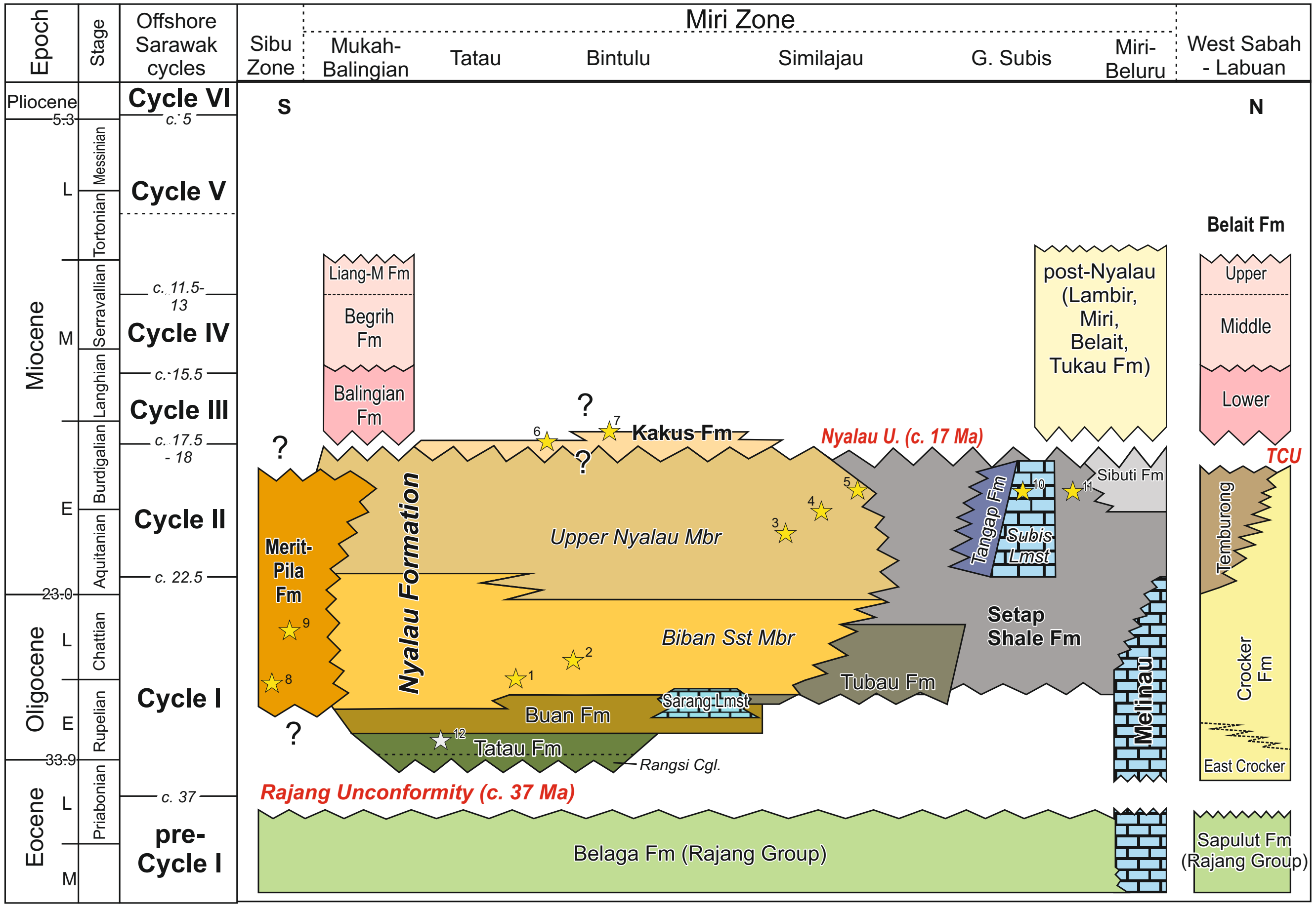
Epoch
Stage
Offshore Sarawak cycles
Sibu Zone
Miri Zone
Mukah-Balingian
Tatau
Bintulu
Similajau
G. Subis
Miri-Beluru
West Sabah - Labuan
S
N
Pliocene
5.3
Miocene
L
M
E
23.0
Oligocene
L
E
33.9
Eocene
L
M
Messinian
Tortonian
Serravallian
Langhian
Burdigalian
Aquitanian
Chattian
Rupelian
Priabonian
Cycle VI
c. 5
Cycle V
c. 11.5-13
Cycle IV
c. 15.5
Cycle III
c. 17.5 - 18
Cycle II
c. 22.5
Cycle I
c. 37
pre-Cycle I
Liang-M Fm
Begrih Fm
Balingian Fm
post-Nyalau (Lambir, Miri, Belait, Tukau Fm)
Belait Fm
Upper
Middle
Lower
TCU
Nyalau U. (c. 17 Ma)
Kakus Fm
Sibuti Fm
Merit-Pila Fm
Nyalau Formation
Upper Nyalau Mbr
Tangap Fm
Subis Lmst
Temburong
Setap Shale Fm
Biban Sst Mbr
Tubau Fm
Melinau
Crocker Fm
Sarang Lmst
Buan Fm
Tatau Fm
Rangsi Cgl.
East Crocker
Rajang Unconformity (c. 37 Ma)
Belaga Fm (Rajang Group)
Sapulut Fm (Rajang Group)

Fig. 3

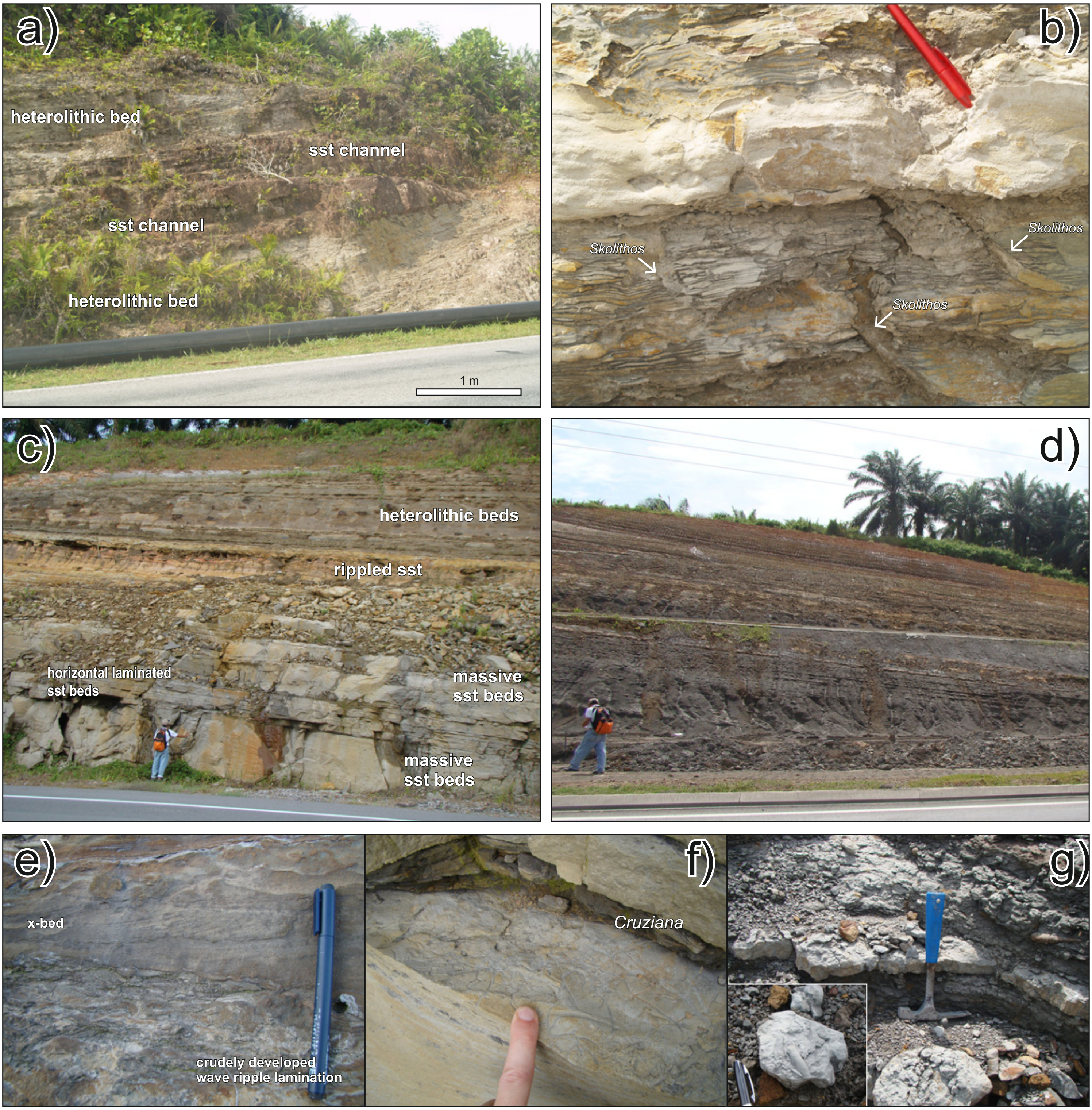
a)
heterolithic bed
sst channel
sst channel
heterolithic bed
1 m
b)
Skolithos
Skolithos
Skolithos
c)
heterolithic beds
rippled sst
horizontal laminated
sst beds
massive
sst beds
massive
sst beds
d)
e)
x-bed
crudely developed
wave ripple lamination
f)
Cruziana
g)

Fig. 4

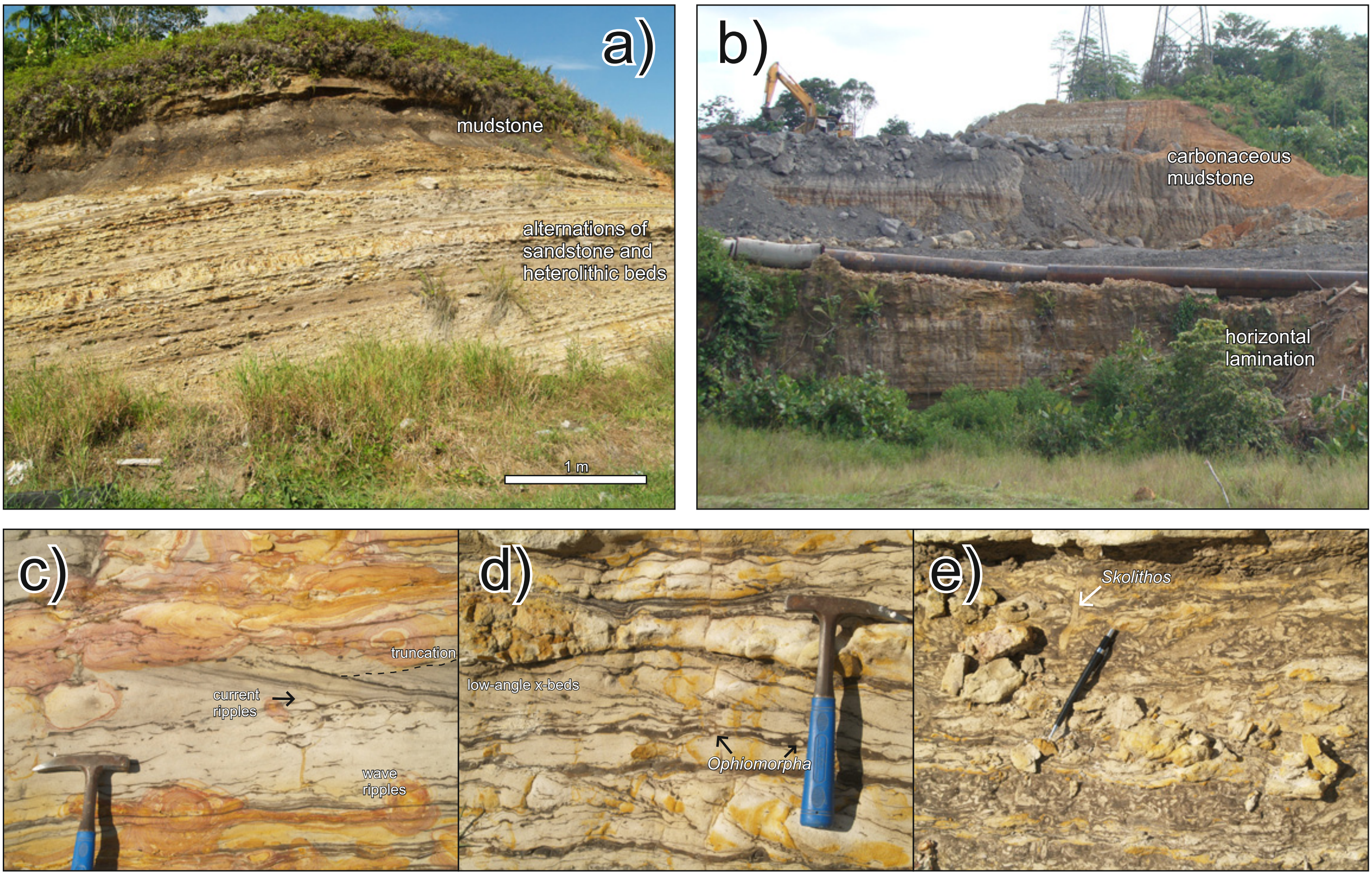
a)
mudstone
alternations of
sandstone and
heterolithic beds
1 m
b)
carbonaceous
mudstone
horizontal
lamination
c)
truncation
current
ripples
wave
ripples
d)
low-angle x-beds
Ophiomorpha
e)
Skolithos

Fig. 5

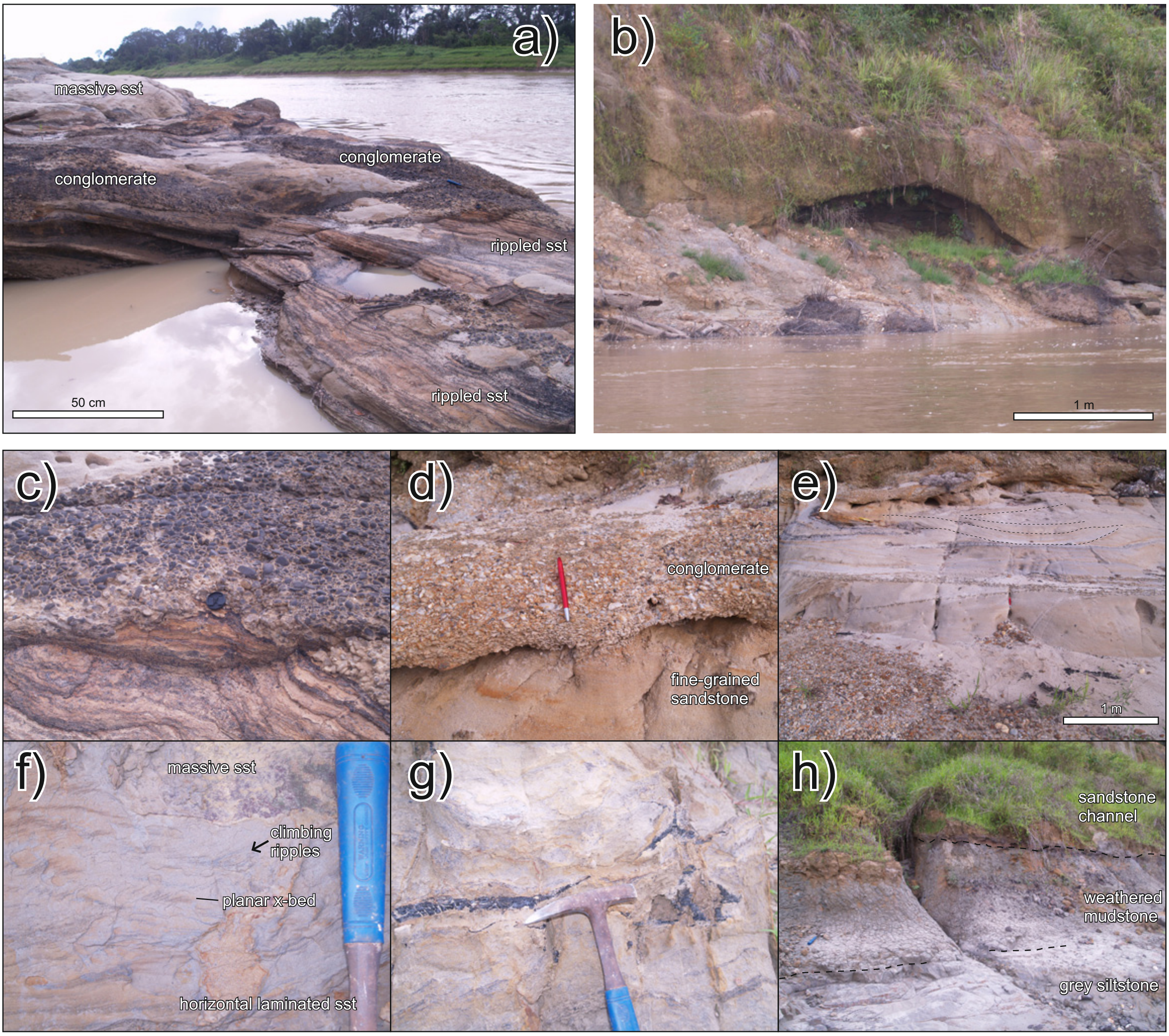
a)
massive sst
conglomerate
conglomerate
rippled sst
rippled sst
50 cm
b)
1 m
c)
d)
conglomerate
fine-grained sandstone
e)
1 m
f)
massive sst
climbing ripples
planar x-bed
horizontal laminated sst
g)
h)
sandstone channel
weathered mudstone
grey siltstone

Fig. 6

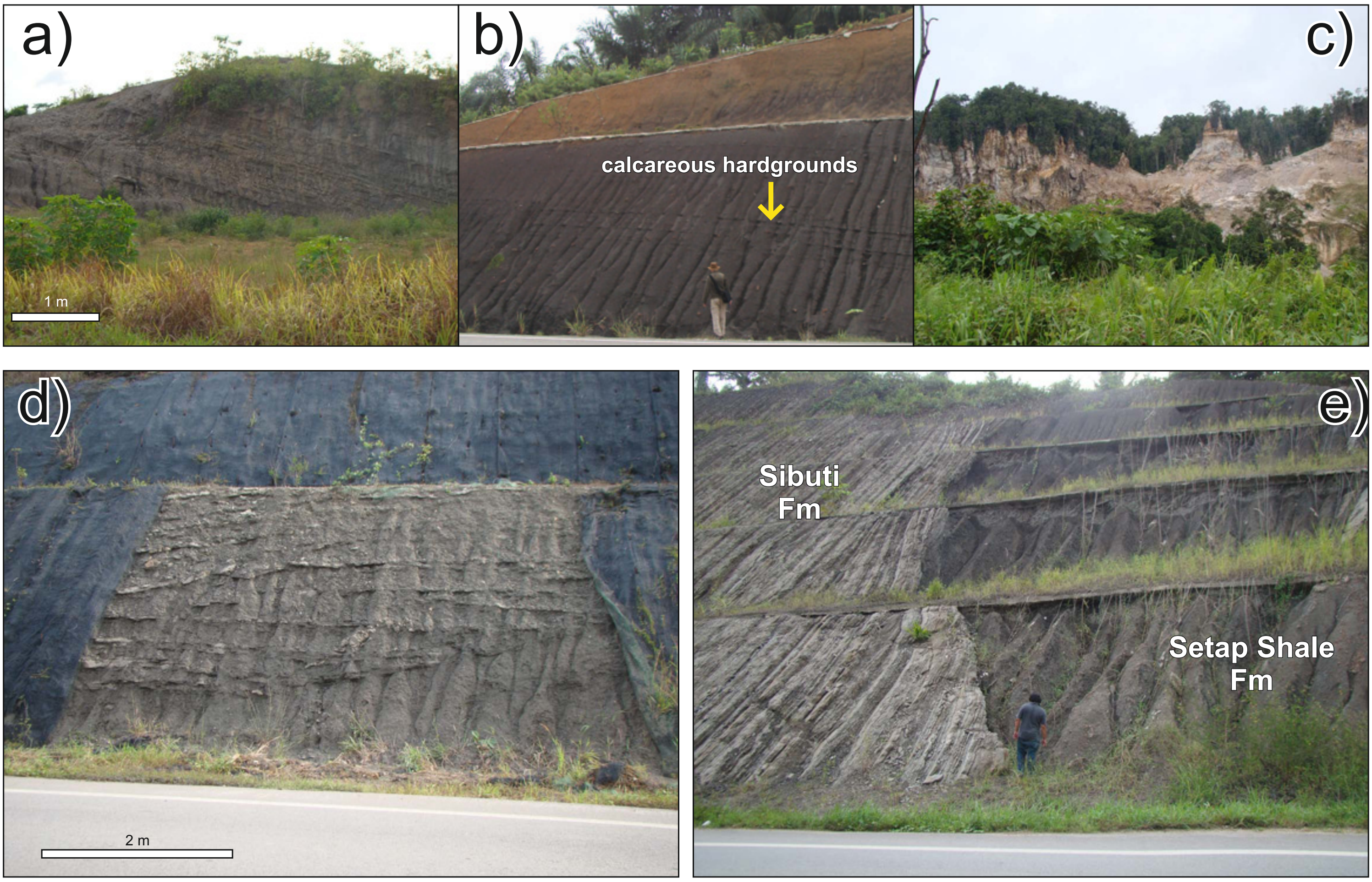
a)
1 m
b)
calcareous hardgrounds
c)
d)
2 m
e)
Sibuti Fm
Setap Shale Fm

Fig. 7

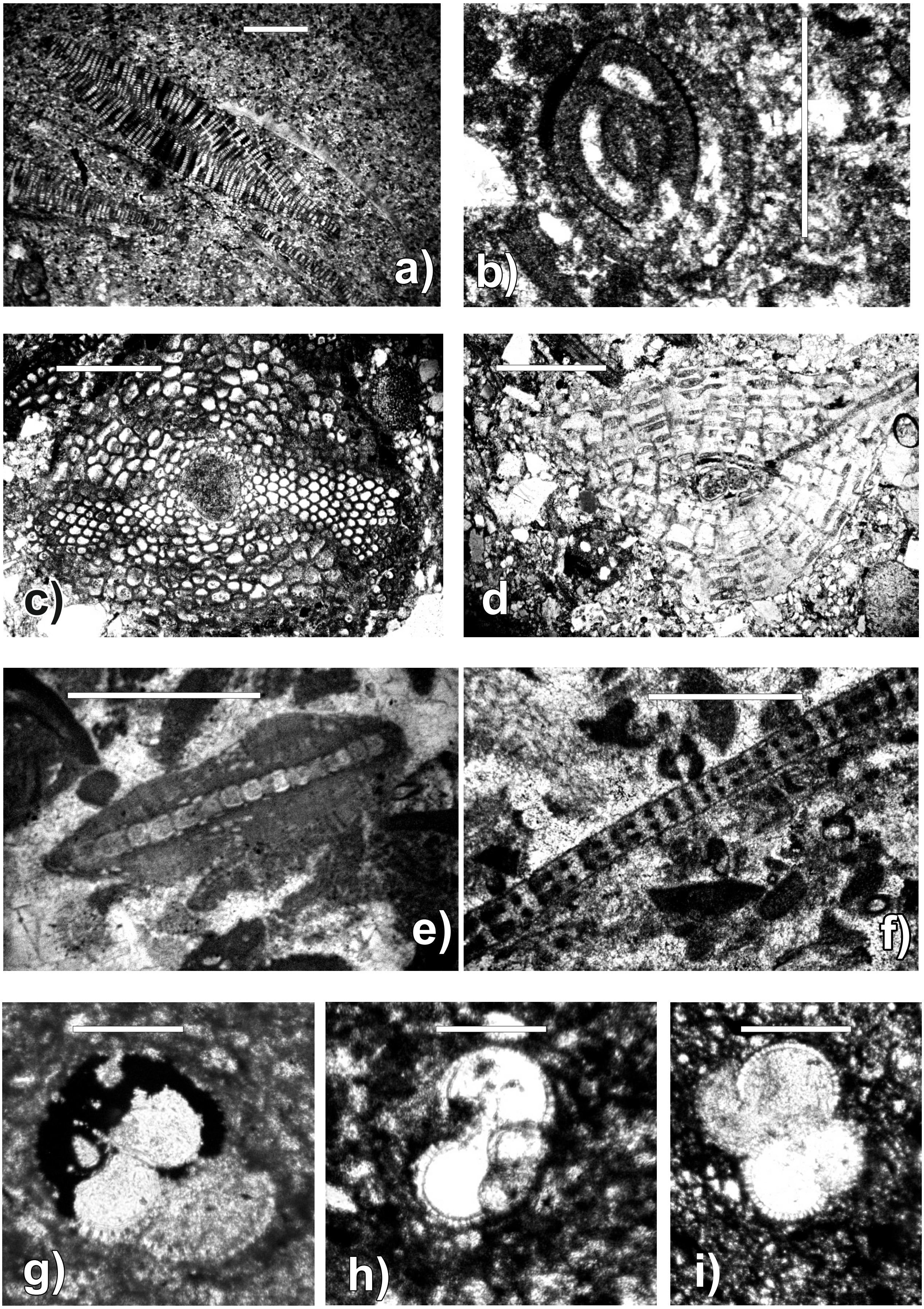
a)
b)
c)
d
e)
f)
g)
h)
i)

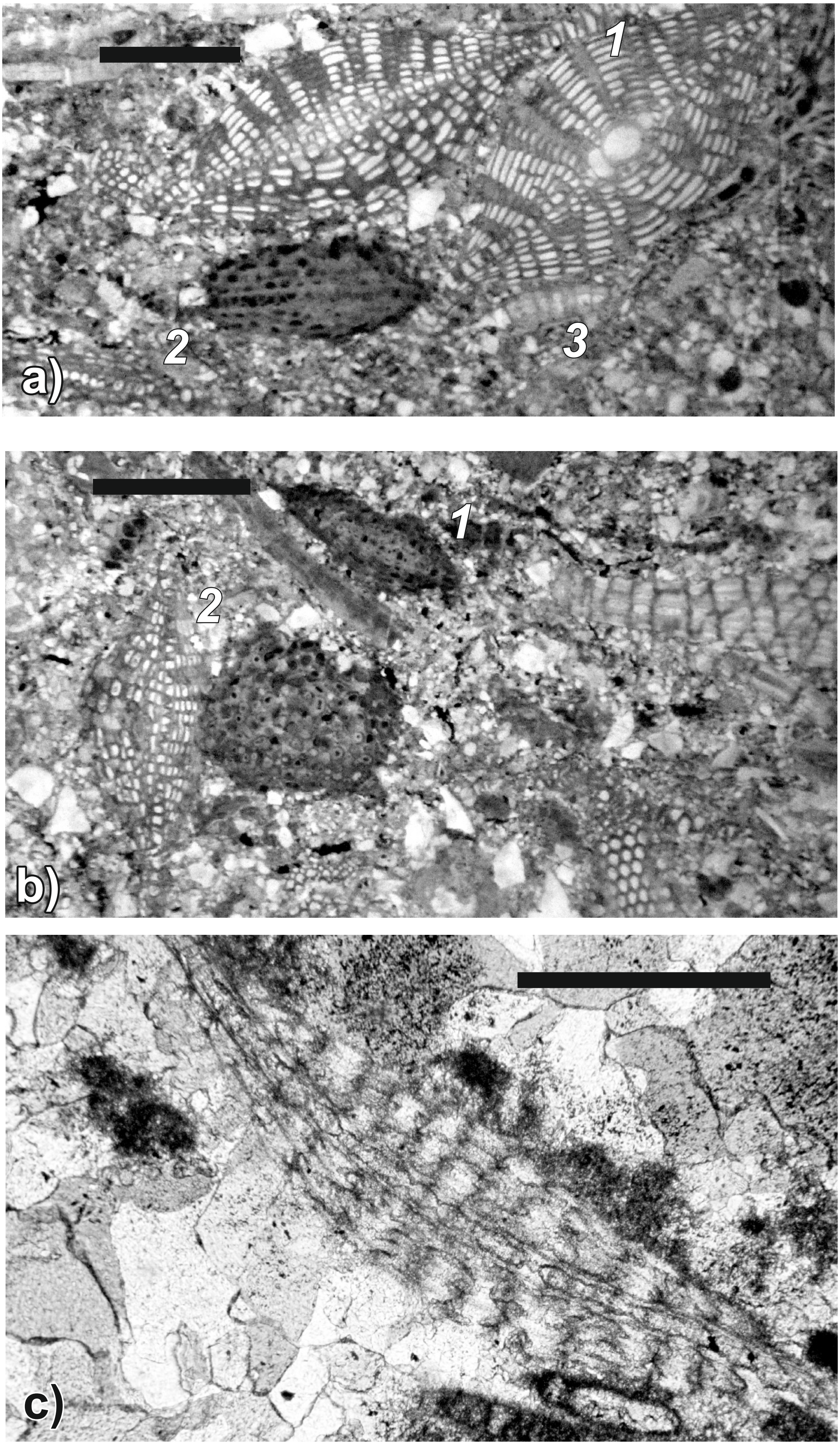
1
2
3
a)
1
2
b)
c)

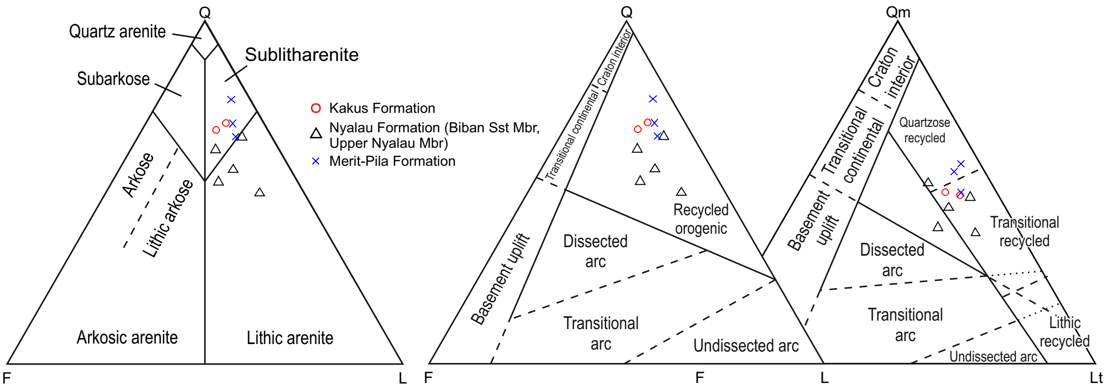

Q
Quartz arenite
Sublitharenite
Subarkose
Kakus Formation
Nyalau Formation (Biban Sst Mbr, Upper Nyalau Mbr)
Merit-Pila Formation
Arkose
Lithic arkose
Arkosic arenite
Lithic arenite
F
L
Q
Craton interior
Transitional continental
Recycled orogenic
Dissected arc
Basement uplift
Transitional arc
Undissected arc
F
F
L
Qm
Craton interior
Transitional continental
Quartzose recycled
Basement uplift
Dissected arc
Transitional recycled
Transitional arc
Lithic recycled
Undissected arc
L
Lt

Fig. 10

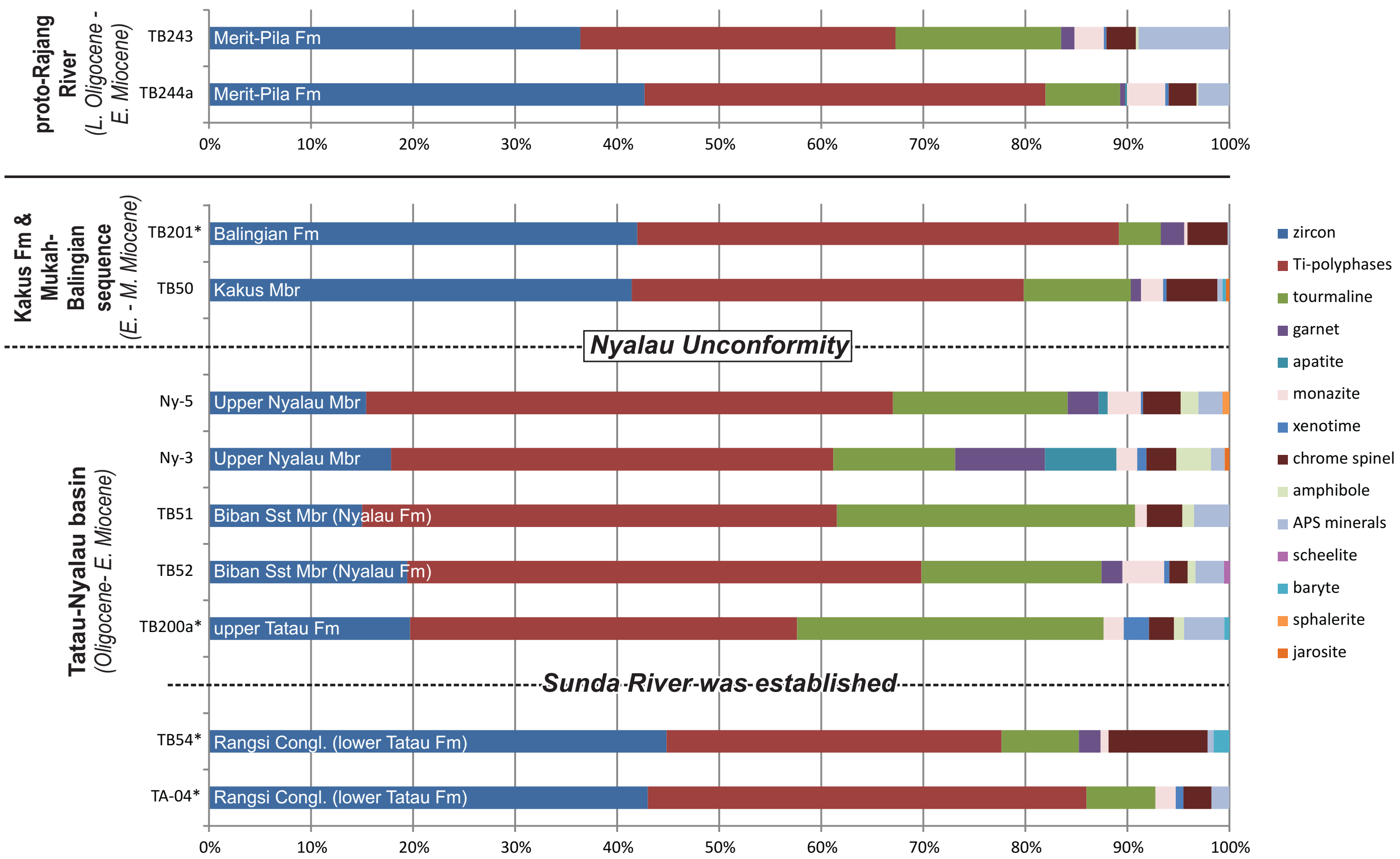

proto-Rajang River
(L. Oligocene - E. Miocene)
TB243
Merit-Pila Fm
TB244a
Merit-Pila Fm
Kakus Fm & Mukah-Balingian sequence
(E. - M. Miocene)
TB201*
Balingian Fm
TB50
Kakus Mbr
Nyalau Unconformity
Tatau-Nyalau basin
(Oligocene- E. Miocene)
Ny-5
Upper Nyalau Mbr
Ny-3
Upper Nyalau Mbr
TB51
Biban Sst Mbr (Nyalau Fm)
TB52
Biban Sst Mbr (Nyalau Fm)
TB200a*
upper Tatau Fm
Sunda River was established
TB54*
Rangsi Congl. (lower Tatau Fm)
TA-04*
Rangsi Congl. (lower Tatau Fm)
0%
10%
20%
30%
40%
50%
60%
70%
80%
90%
100%
zircon
Ti-polyphases
tourmaline
garnet
apatite
monazite
xenotime
chrome spinel
amphibole
APS minerals
scheelite
baryte
sphalerite
jarosite

Fig. 11

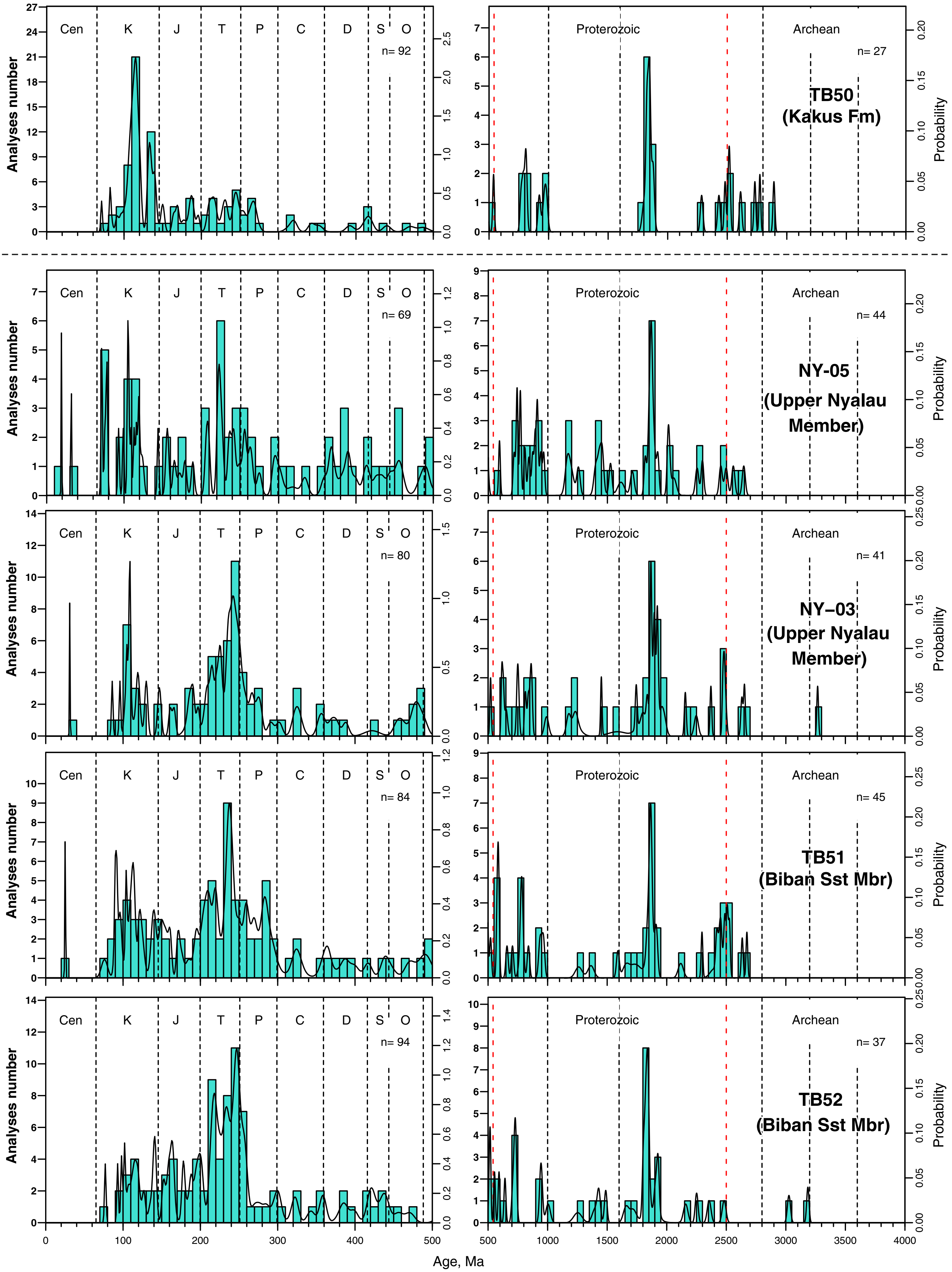

Analyses number
Probability
Cen
K
J
T
P
C
D
S
O
Proterozoic
Archean
n= 92
n= 27
TB50
(Kakus Fm)
n= 69
n= 44
NY-05
(Upper Nyalau
Member)
n= 80
n= 41
NY–03
(Upper Nyalau
Member)
n= 84
n= 45
TB51
(Biban Sst Mbr)
n= 94
n= 37
TB52
(Biban Sst Mbr)
Age, Ma

Fig. 12

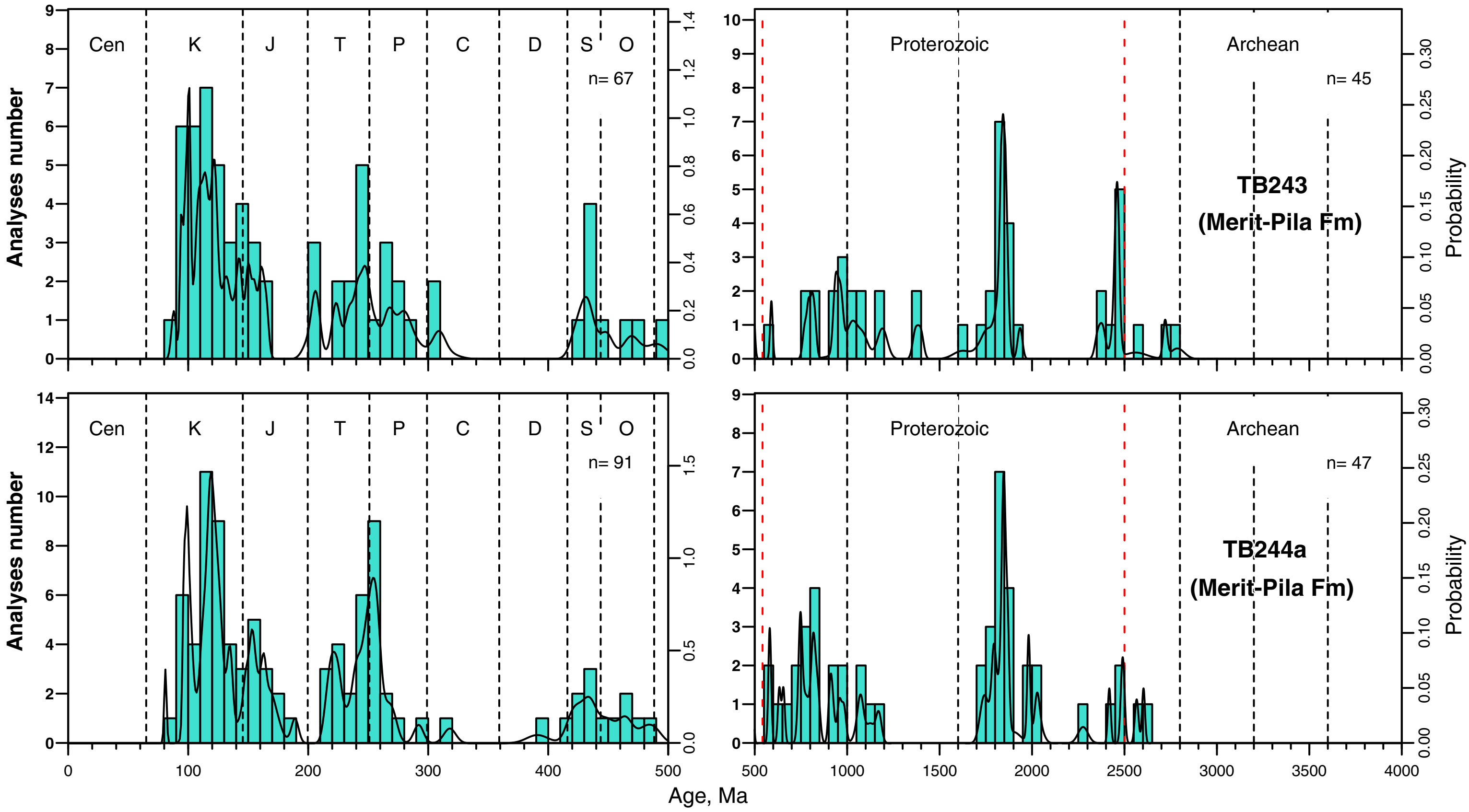

Analyses number
Probability
Cen
K
J
T
P
C
D
S
O
n= 67
n= 91
Proterozoic
Archean
n= 45
n= 47
TB243
(Merit-Pila Fm)
TB244a
(Merit-Pila Fm)
Age, Ma

Fig. 13

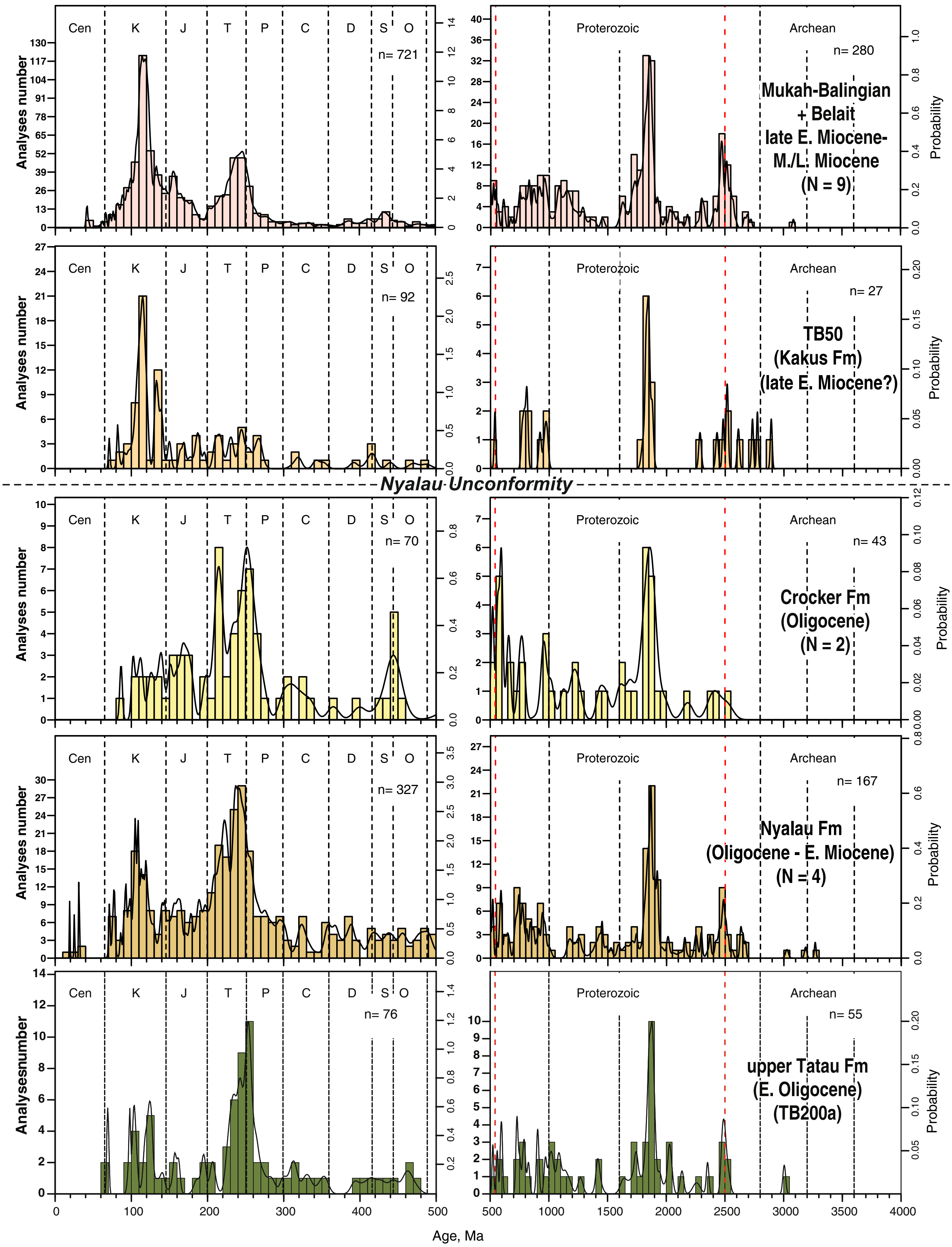

Cen
K
J
T
P
C
D
S
O
Proterozoic
Archean
n= 721
n= 280
Mukah-Balingian + Belait late E. Miocene- M./L. Miocene (N = 9)
n= 92
n= 27
TB50 (Kakus Fm) (late E. Miocene?)
Nyalau Unconformity
n= 70
n= 43
Crocker Fm (Oligocene) (N = 2)
n= 327
n= 167
Nyalau Fm (Oligocene - E. Miocene) (N = 4)
n= 76
n= 55
upper Tatau Fm (E. Oligocene) (TB200a)
Analyses number
Analysesnumber
Probability
Age, Ma

Fig. 14

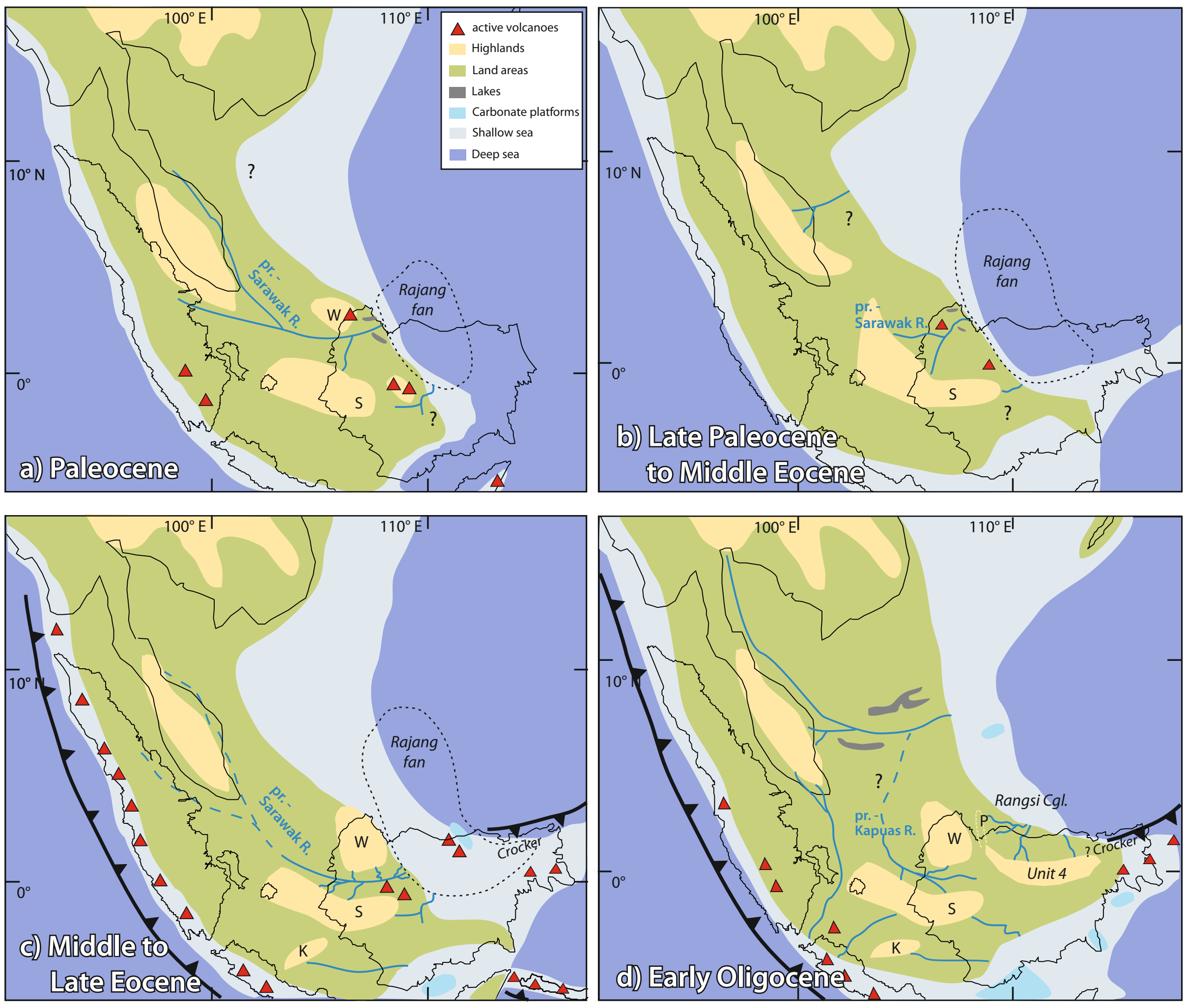

a) Paleocene
b) Late Paleocene to Middle Eocene
c) Middle to Late Eocene
d) Early Oligocene
active volcanoes
Highlands
Land areas
Lakes
Carbonate platforms
Shallow sea
Deep sea
100° E
110° E
10° N
0°
pr.-Sarawak R.
pr.-Kapuas R.
Rajang fan
Crocker
Rangsi Cgl.
Unit 4
W
S
K
P

Fig. 15

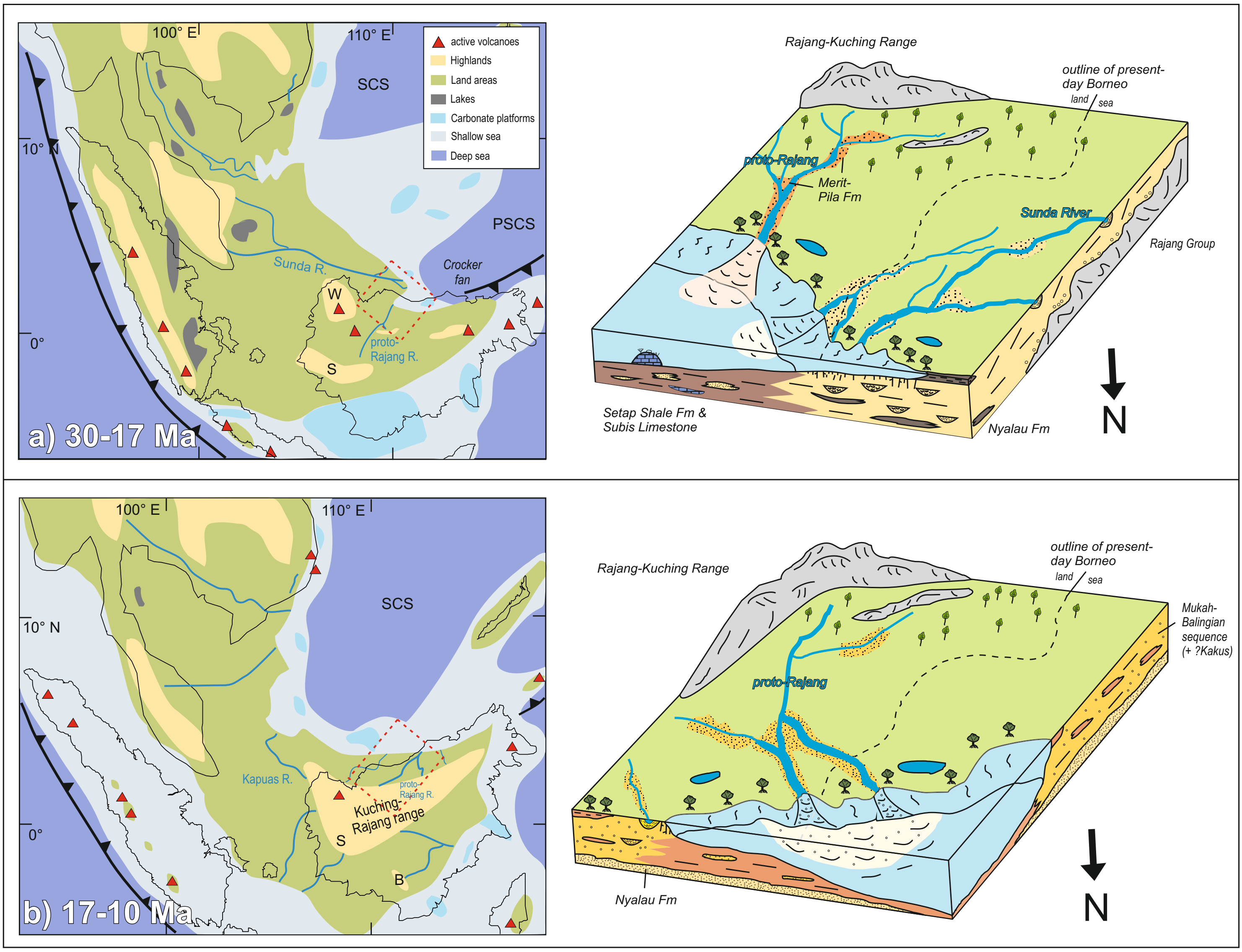
active volcanoes
Highlands
Land areas
Lakes
Carbonate platforms
Shallow sea
Deep sea
100° E
110° E
10° N
0°
SCS
PSCS
Sunda R.
Crocker fan
W
S
proto-Rajang R.
a) 30-17 Ma
Rajang-Kuching Range
outline of present-day Borneo
land
sea
proto-Rajang
Merit-Pila Fm
Sunda River
Rajang Group
Setap Shale Fm & Subis Limestone
Nyalau Fm
N
Kapuas R.
Kuching-Rajang range
B
b) 17-10 Ma
Mukah-Balingian sequence (+ ?Kakus)

Fig. 16